Atomic Physics

Correlated processes in the inner-shell photodetachment of the Na^- ion
Covington, A.M., A. Aguilar, V.T. Davis, I. Alvarez, H.C. Bryant, C. Cisneros, M. Halka, D. Hanstorp, G. Hinojosa, A.S. Schlachter, J.S. Thompson, D.J. Pegg

Dynamical relativistic effects in photoionization: Spin-orbit-resolved angular distributions of xenon *4d* photoelectrons near the Cooper minimum
Hemmers, O., H. Wang, G. Snell, M.M. Sant' Anna, I. Sellin, N. Berrah, D.W. Lindle, P.C. Deshmukh, N. Haque, S.T. Manson

Excitation-energy dependence of Cu $L_{2,3}$ x-ray spectra of Cu, Cu_2O and CuO
Kawatsura, K., K. Takahiro, N. Takeshima, T. Morikawa, Y. Muramatsu, R.C.C. Perera

First separate measurements of the nondipole parameters γ and δ: Showcase neon 2p photoemission
Hemmers, O., M. Blackburn, T. Goddard, P. Glans, H. Wang, S.B. Whitfield, R. Wehlitz, I.A. Sellin, D.W. Lindle

High resolution photoionization measurements of Mg^+ and Al^+ ions
Aguilar, A., J.B. West, R.A. Phaneuf, H. Kjeldsen, F. Folkmann, J.D. Bozek, A.S. Schlachter, C. Cisneros

K-shell photodetachment of Li^-: Experiment and theory
Bozek, J.D., A.A. Wills, G. Turri, G. Akerman, B. Rude, H.-L. Zhou, S.T. Manson, N.D. Gibson, C.W. Walter, L. Vo Ky, A. Hibbert, R.A. Phaneuf, S.M. Ferguson, N. Berrah

K-shell photoexcitation of carbon ions: lifetime of a K-shell vacancy
Schlachter, A.S., M.M. Sant' Anna, A.M. Covington, A. Aguilar, M.F. Gharaibeh, G. Hinojosa, R.A. Phaneuf, I. Alvarez, C. Cisneros, A. Müller, B.M. McLaughlin

Mechanisms of photo double ionization of helium by 530 eV photons
Knapp, A., A. Kheifets, I. Bray, Th. Weber, A.L. Landers, S. Schössler, T. Jahnke, J. Nickles, S. Kammer, O. Jagutzki, L.Ph. Schmidt, T. Osipov, J. Rösch, M.H. Prior, H. Schmidt-Böcking, C.L. Cocke, R. Dörner

Mirroring doubly excited resonances in neon
Canton, S.E., A.A. Wills, T.W. Gorczyca, M. Wiedenhoeft, E. Sokell, J.D. Bozek, G. Turri, X. Feng, N. Berrah

Photoionization of C^{2+} ions
Müller, A., R.A. Phaneuf, A. Aguilar, M.F. Gharaibeh, A.S. Schlachter, I. Alvarez, C. Cisneros, G. Hinojosa, B.M. McLaughlin

Photoionization of doubly charged scandium ions
Schippers, S., A. Müller, S. Ricz, M.E. Bannister, G.H. Dunn, J. Bozek, A.S. Schlachter, G. Hinojosa, C. Cisneros, A. Aguilar, A. Covington, M. Gharaibeh, R.A. Phaneuf

Photoionization of Ne^+: An absolute benchmark for theory
Covington, A.M., A. Aguilar, I. Álvarez, J.D. Bozek, C. Cisneros, I.R. Covington, I. Dominguez, M.F. Gharaibeh, G. Hinojosa, B.M. McLaughlin, M.M. Sant' Anna, A.S. Schlachter, C.A. Shirley, R.A. Phaneuf

Soft x-ray emission spectroscopy of ions in solution
Augustsson, A., J.-H. Guo, D. Spandberg, K. Hermansson, J. Nordgren

Correlated Processes in the Inner-Shell Photodetachment of the Na^- Ion

A. M. Covington[1], A. Aguilar[1], V. T. Davis[2], I. Alvarez[3], H. C. Bryant[4], C. Cisneros[3], M. Halka[5], D. Hanstorp[6], G. Hinojosa[3], A. S. Schlachter[7], J. S. Thompson[1]and D. J. Pegg[8]

[1]Department of Physics and Chemical Physics Program,University of Nevada, Reno, Nevada 89557-0058, USA
[2]Department of Physics, United States Military Academy, West Point, NY 10996, USA
[3]Centro de Ciencias Fisicas UNAM, Apdo. Postal 48-3 CP 62251 Cuernavaca , Mor. Mexico
[4]Physics and Astronomy, University of New Mexico, Albuquerque, NM 87131, USA
[5]Department of Physics, Portland State University, P.O. Box 751, Portland, Oregon 97229, USA
[6]Department of Physics, Chalmers University of Technology and Goteborg University, SE-412 96 Goteborg Sweden
[7]Lawrence Berkeley National Laboratory, 1 Cyclotron Road, Berkeley, CA 94720, USA
[8]Department of Physics, University of Tennessee, Knoxville, TN 37996, USA

Photodetachment studies of negative ions have, until recently, involved the valence electrons only. Double excitation, a clear sign of the importance of electron correlation, has been investigated extensively during the past few decades[1]. Such measurements used lasers as the source of UV photons. At much higher levels of excitation, one can expect to observe thresholds and resonances in the photodetachment cross section arising from the detachment and/or excitation of an inner-shell electron. To reach these high levels of excitation, which in the present case lie in the XUV region, it is necessary to replace lasers with a synchrotron radiation source. The present experiment was performed on the photon-ion endstation 10.0.1.2 at the 10.0.1 beamline at the Advanced Light Source.

In the experiment we collinearly overlapped a beam of Na^- ions from a low-energy accelerator with a beam of XUV photons from the ALS. Na^- ions were produced in a sputter ion source, extracted at an energy of 5 keV and focused using a series of cylindrical electrostatic lenses. The ion beam was momentum-selected using a 60^o analyzing magnet. The cross sectional area of the ion beam was defined by two sets of adjustable slits. After momentum-selection and collimation, the ion beam was merged onto the axis of a counter-propagating photon beam using a set of 90^o spherical-sector bending plates. The primary beam then entered a 29.4 cm long cylindrical interaction region which was biased at +2 kV to energy label the Na^+ ions produced as a result of the photon-ion interactions. The energy labeling of these photo-ions enabled us to distinguish them from the Na^+ ions produced in double detachment collisions of the Na^- ions with the residual gas along the unbiased region of the ion beam line. This background contribution was also reduced by maintaining a vacuum of $5x10^{-10}$ Torr in the beam line. After the interaction region, a 45^o analyzing magnet was used to separate the energy-labeled Na^+ ions produced in the biased interaction region from the primary Na^- ion beam. These ions had an energy of 9 keV, whereas most of the collisionally detached background ions had an energy of 5 keV, as determined by the extraction voltage at the ion source. Typical Na^- ion currents in the interaction region were 1-6 nA. The magnitudes of the ion current and photon intensity were monitored for normalization purposes. The photon beam was modulated at 1 Hz in order to discriminate against the collisionally-induced background of 9 keV Na^+ ions produced in the interaction region. The Na^+ photo-ions were further deflected, in the vertical dispersion plane, by the use of a set of 90^o spherical-sector bending plates. This was to minimize any background arising from the collection of the Na^- primary beam. The dispersed Na^+ photo-ions then entered a negatively-biased detection box, where the ions impinged on a metal plate and produced secondary electrons. These secondary electrons were, in turn, accelerated toward a microchannel plate detector. The processed pulses from this detector were counted with a multi-function I/O board in a PC-based data acquisition and control system. The Na^+ signal, which is proportional

to the cross section, is shown, as a function of photon energy, in Figure 1. This figure is made up of two data sets taken under different conditions and smoothed separately. In the range 30-40 eV, the resolution and step size were 40 meV and 6 meV, respectively. In the range 40-51 eV the resolution and step size were both 100 meV. Further details can be found in a recent publication [2].

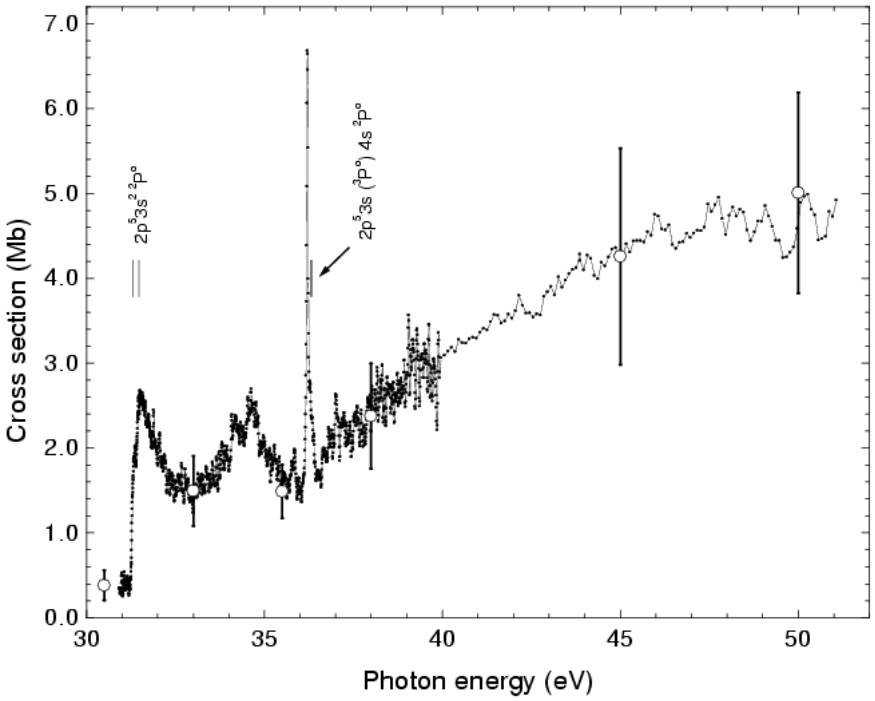

Figure 1 Total cross section for photodetachment of Na^- over energy range 30-51 eV. The six measurements represented by open circles were used to establish the cross-section scale. The scale shown is a lower limit. Thresholds are indicated by vertical lines.

Figure 1 shows the photodetachment cross section of the Na^- ion leading to the production of the Na^+ ion. In the measured energy range 30-51 eV, two distinct processes contribute to the cross section. There is the non-resonant process involving the direct photodetachment of a 2p electron from Na^- producing Na atoms in core-excited states, which rapidly decay via Auger emission to form Na^+ ions. The first channel to open is the $Na(2p^5 3s^2)^2P^o + e^-$ channel. The fine structure channels associated with the $^2P^o$ levels can be clearly seen. The sharp opening of this channel is expected for dominant s-wave emission. This channel is the most prominent non-resonant channel over the energy range studied. The cross rises gradually from threshold to a maximum slightly beyond the range of our measurements. At higher energies, detachment of the 2p electron is often accompanied by the excitation of a valence electron. Resonant processes are also apparent in the cross section. The resonances arise from photoexcitation of core-excited states of the Na^- ion of $^1P^o$ symmetry, which subsequently decay via autodetachment to corresponding core-excited states of the Na atom. The excited Na atoms then decay via the Auger process to produce Na^+ ions. The probability of radiative decay to the bound states should be very small. The most prominent feature of the cross section in the

range studied is the Na^- resonance at 36.213 eV. This narrow peak lies very close to the threshold for the opening of the $Na(2p^5 3s(^3P^o)4s)^2P^o + e^-$ channel. It is most likely associated with the autodetaching decay of a core-excited $^1P^o$ state of Na^- with a major configuration of the type $2p^5 3s4snl$, where l is even. The resonance appears to be just below the parent threshold. Feshbach resonances, such as this, are known to narrow as they approach their parent threshold. The strength of the prominent Na^- resonance, in comparison to corresponding resonances in Na, clearly demonstrates the much higher degree of correlation associated with double excitation process in the negative ion than in the atom. Other, weaker resonances, have been observed in the cross section. Details can be found in reference [2].

We would like to take this opportunity to thank Professor Ronald Phaneuf for permitting us to use the collinear beams apparatus situated at the 10.0.1.2 endstation at ALS. This apparatus was constructed at the University of Nevada, Reno under the direction of Dr Phaneuf. The work at ALS is supported by the US Department of Energy under contract DE-AC03-76SF00098. We would like to acknowledge support of A.C. and A.A. and the endstation by the Division of Chemical Sciences, Biosciences and Geosciences of the US Department of Energy under contract DE-FG03-ER14787 with the U. Nevada, Reno. I.A., C.C., G.H., and A.A. acknowledge support from DGAPA-UNAM and CONACyT. D.H acknowledges support from the Swedish Research Council. We would like to thank Brendan McLaughlin for valuable discussions.

References

[1]. For example, P.Harris et al., Phys. Rev.A 42,6443(1990); G.Haeffler et al., Phys. Rev. A 59, 3655(1999); I.Kiyan et al., Phys. Rev. Letters, 81, 2874 (1998).
[2]. A.M.Covington et al., J.Phys.B 34, L735(2001).

Contact Information:

Dr. David J. Pegg
401 Nielsen Physics Building
The University of Tennessee
Knoxville, TN 37996-1200
Phone: 865-974-7831
FAX: 865-974-7843
Email: djpegg@utkux.utk.edu

Dynamical Relativistic Effects in Photoionization: Spin-Orbit-Resolved Angular Distributions of Xenon 4*d* Photoelectrons near the Cooper Minimum

O. Hemmers,[1] H. Wang,[1,2] G. Snell,[3,4] M. M. Sant'Anna,[4] I. Sellin,[5] N. Berrah,[3]
D. W. Lindle,[1] P.C. Deshmukh,[6,7,8] N. Haque,[9] and S. T. Manson[7]
[1]Department of Chemistry, University of Nevada, Las Vegas, NV 89154-4003
[2]Department of Physics, Uppsala University, Box 530, S-751 21 Uppsala, Sweden
[3]Department of Physics, Western Michigan University, Kalamazoo, MI 49008-5151
[4]Advanced Light Source, Lawrence Berkeley National Laboratory, Berkeley, California 94720, USA
[5]Department of Physics, University of Tennessee, Knoxville, TN 37996
[6]Department of Physics, Indian Institute of Technology-Madras, Chennai 600036, India
[7]Department of Physics and Astronomy, Georgia State University, Atlanta, GA 30030
[8]Center for Theoretical Studies of Physical Systems, Clark-Atlanta University, Atlanta, GA 30314
[9]Department of Physics, Morehouse College, Atlanta, GA 30314

INTRODUCTION

Relativistic effects in atoms have long been known to be important for photoionization dynamics at high **Z** [1,2]. At low and intermediate **Z**, where the predominant effect of relativity has been thought to be spin-orbit splitting of states into $j=l\pm1/2$ with differing threshold energies [1], recent advances in experiment [3] and theory [4] have demonstrated observable consequences of relativistic effects on photoionization dynamics. One of the most sensitive dynamical quantities in photoionization is the energy of a Cooper minimum, where the dipole matrix element for a particular channel goes through (or nearly goes through) zero. Relativistic interactions were predicted to significantly affect Cooper minima two decades ago [2]. Here, we report on a combined experimental and theoretical study of 4*d* photoionization in Xe where the spin-orbit components $4d_{5/2}$ and $4d_{3/2}$ are individually resolved. Experimentally this is difficult in the energy region of the $4d\rightarrow\varepsilon f$ Cooper minima because the dominant $d\rightarrow f$ contribution to the cross section is very small. In the absence of dynamical effects due to relativistic interactions, Cooper minima for $4d_{5/2}$ and $4d_{3/2}$ photoionization will be located at the same *kinetic energy*. Consequently, $\beta_{5/2}$ and $\beta_{3/2}$ would be identical as a function of photoelectron energy. However, the present measurements clearly exhibit differences in the β parameters and confirm the long-untested theoretical prediction of Kim *et al.* [2]. Furthermore, $\beta_{5/2}$ and $\beta_{3/2}$ differ not only in the immediate vicinity of the Cooper minima, but over a broad energy region, demonstrating the importance of relativistic effects in the photoionization of intermediate-**Z** atoms over a much larger energy range than previously suspected. The $4d\rightarrow\varepsilon f$ non-relativistic Cooper minimum splits into three minima relativistically; $4d_{5/2}\rightarrow\varepsilon f_{5/2}$, $4d_{5/2}\rightarrow\varepsilon f_{7/2}$ *and* $4d_{3/2}\rightarrow\varepsilon f_{5/2}$. Each would appear at the same photoelectron energy in the absence of dynamical effects resulting from relativistic interactions.

EXPERIMENTS

To check possible systematic errors related to a particular experimental method, the measurements were done independently with hemispherical and time-of-flight (TOF) electron spectrometers at two different undulator beamlines at the Advanced Light Source (ALS) at Lawrence Berkeley National Laboratory. One experiment was carried out at beamline 10.0.1 using an endstation designed for gas-phase angle-resolved studies based on the Scienta SES-200 hemispherical electron analyzer (HEA) [5]. The analyzer is rotatable in the perpendicular plane,

allowing electron angular-distribution studies. Measurements at the θ angles of 0°, 54.7° and 90° were performed, and angular-distribution parameters were determined. In the TOF measurements, performed at ALS beamline 8.0, two analyzers are mounted in the perpendicular plane at θ=0° and θ=54.7°, allowing simultaneous measurements for accurate determination of β parameters [6]. To determine β parameters, the data were calibrated with the Ne-2*s* photoline, which has a fixed β value of 2. In both experiments, for most of the data, the photon energy was increased in 2-eV steps, because the energy splitting of the spin-orbit components is 2.0 eV. This approach permitted the measurement of $\beta_{5/2}$ and $\beta_{3/2}$ at the same photoelectron *kinetic energy*, and the difference $\beta_{3/2}$-$\beta_{5/2}$ could be calculated easily. At higher energies, where larger energy steps were used (TOF measurements only), continuous curves were interpolated through the measured values of β and used to estimate the difference $\beta_{3/2}$-$\beta_{5/2}$.

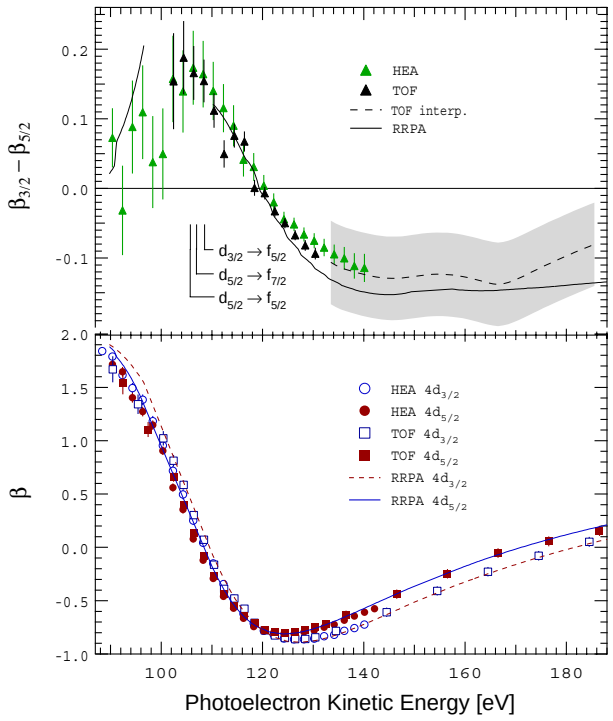

Figure 1. Lower panel: Photoelectron angular-distribution parameters, $\beta_{5/2}$ and $\beta_{3/2}$, for Xe 4*d* ionization as a function of photoelectron energy. The points are the present experiment and the curves are our theoretical results. Upper panel: $\beta_{3/2}$-$\beta_{5/2}$ as a function of photoelectron energy derived from the data in the lower panel. The dashed curve was obtained via interpolation of the TOF data, and the shaded area represents error bars. Omitted from theory is the region of the $4p \rightarrow ns,nd$ resonances. Also shown are theoretical predictions for the locations of the Cooper minima.

RESULTS

Calculations were performed using the relativistic random-phase approximation (RRPA) [7] based upon the Dirac Equation; relativistic effects are included on an *ab initio* basis. All relativistic single-excitation channels from the 4*s*, 4*p*, 4*d*, 5*s* and 5*p* subshells were included in the calculation, a total of 20 interacting channels. As noted above, in the absence of relativistic effects, β_j *must* be independent of j as a function of photoelectron energy. The present results for $\beta_{5/2}$ and $\beta_{3/2}$ as a function of photoelectron energy are shown in the lower panel of Fig. 1, where a clear difference is evident. To focus on this difference more clearly, values of $\beta_{3/2}$-$\beta_{5/2}$ are shown in the upper panel of Fig. 1, where zero corresponds to the nonrelativistic expectation. Also shown in Fig. 1 are the results of our RRPA calculations. The agreement is remarkably good between theory and experiment. The part missing from the theoretical curve is the $4p \rightarrow ns,nd$ resonance region where the theoretical results are affected by autoionization. There is also excellent agreement between the two sets of experimental results, providing confidence in the reliability of the measurements. Note particularly that the β-parameter curves are not simply shifted, but have different shapes, *e.g.*, $\beta_{3/2}$ goes lower than $\beta_{5/2}$, and the differences persist to higher energy. At still higher energies, recent work has shown that interchannel interactions are pervasive and often dominant for most subshells of most atoms at most energies [8], so much so

that even the asymptotic form of the high-energy nonrelativistic photoionization cross section for non-*s*-states is altered. Thus, as long as 4*d* photoionization does not dominate the total cross section, significant interchannel interactions will modify the 4*d* transition amplitudes. But there is no reason to expect these interchannel interactions will modify each relativistic amplitude in the same way, *i.e.*, interchannel coupling will cause observable differences between $\beta_{3/2}$ and $\beta_{5/2}$ for *all* higher energies. Near threshold, it is also known $\beta_{3/2}$ and $\beta_{5/2}$ differ due to differing exchange interactions among the relativistic channels. Only in the shape-resonance region, 30-80-eV kinetic energy, are there no differences between $\beta_{3/2}$ and $\beta_{5/2}$, because the 4*d* cross section dominates here and the energy is high enough so exchange interactions are no longer important; interchannel interactions are negligible *only* in this narrow region. Thus, except for a small energy region near the 4*d* shape resonance, equality of $\beta_{3/2}$ and $\beta_{5/2}$ is the exception, not the rule.

CONCLUSIONS

Finally, there is no reason to suspect Xe 4*d* is a special case; the results found in this work should be quite general. We thus expect effects of relativistic interactions on interchannel coupling will be widespread over all intermediate-**Z** atoms. These effects also should be manifest in clusters, molecules, surfaces, and solids.

ACKNOWLEDGMENTS

The authors thank the staff of ALS for their support during the experiments.

REFERENCES

1. S. T. Manson, C. J. Lee, R. H. Pratt, I. B. Goldberg, B. R. Tambe, and A. Ron, Phys. Rev. A **28**, 2885 (1983).
2. Y. S. Kim, A. Ron, R. H. Pratt, B. R. Tambe and S. T. Manson, Phys. Rev. Lett. **46**, 1326 (1981).
3. G. S. Canton-Rogan, A. A. Wills, T. W. Gorczyca, M. Wiedenhöft, O. Nayandin, C. N. Liu and N. Berrah, Phys. Rev. Lett. **85**, 3113 (2000).
4. H. S. Chakraborty, A. Gray, J. T. Costello, P. C. Deshmukh, G. N. Haque, E. T. Kennedy, S. T. Manson and J.-P. Mosnier, Phys. Rev. Lett. **83**, 2151 (1999).
5. N. Berrah, B. Langer, A. Wills, E. Kukk, J. D. Bozek, A. Farhat and T. W. Gorczyca, J. Electron Spectrosc. & Relat. Phenom. **101-103**, 1 (1999).
6. O. Hemmers, S. B. Whitfield, P. Glans, H. Wang, D.W. Lindle, R. Wehlitz, and I. A. Sellin, Rev. Sci. Instrum. **69**, 3809 (1998).
7. W. R. Johnson and C. D. Lin, Phys. Rev. A **20**, 964 (1979).
8. D. L. Hansen, O. Hemmers, H. Wang, D. W. Lindle, I. A. Sellin, H. S. Chakraborty, P. C. Deshmukh and S. T. Manson, Phys. Rev. A **60**, R2641 (1999).

This work was supported by the DOE, Office of Science, BES, DOE EPSCoR, NSF, NASA and CNPq, Brazil. The ALS is funded by the DOE, Materials Sciences Division, Basic Energy Sciences, under Contract No. DE-AC03-76SF00098.

Principal investigator: Dennis Lindle, Department of Chemistry, University of Nevada, Las Vegas, NV 89154-4003. Email: lindle@unlv.edu. Telephone: 702-895-4426.

This work has been published in Phys. Rev. Lett. **87**, 123004 (2001).

Excitation-Energy Dependence of Cu $L_{2,3}$ X-Ray Emission Spectra of Cu, Cu_2O and CuO

K. Kawatsura[1], K. Takahiro[1], N. Takeshima[1], T. Morikawa[1], Y. Muramatsu[2] and R.C.C. Perera[3]

[1] Department of Chemistry and Materials Technology, Kyoto Institute of Technology, Sakyo-ku, Kyoto 606-8585, Japan

[2] Synchrotron Radiation Center, Kansai Research Establishment, Japan Atomic Energy Research Institute, 1-1-1 Kouto, Mikazuki, Hyogo 679-5148, Japan

[3] Center for X-Ray Optics, Lawrence Berkeley National Laboratory, 1 Cyclotron Road, Berkeley, California 94720, USA

INTRODUCTION

Cu metal and its oxides have recently attracted considerable attention for the study of the electronic structure of copper oxides based on the superconducting matters. The Cu *L* X-ray emission spectra of Cu metal and its oxides have been measured by many laboratories for studying the electronic structure of the valence bands and the effect of chemical bonding on the satellites structure of the main peak of Cu $L\alpha_{1,2}$ X-ray emission using usual X-ray source [1,2] and synchrotron radiation [3-5]. The incident photon energy dependence was measured for Cu $L_{2,3}$ satellites using synchrotron radiation [3-5]. Changes in the Cu $L_{2,3}$ X-ray emission spectra with Cu metal and its oxides have been measured using electron excitation by Fischer [6]. He found that relative intensity $L\beta_1/L\alpha_{1,2}$ significantly depends on the incident electron energy and the target. The relative intensity $L\beta_1/_{L\alpha 1,2}$ decreases with increase of excitation energy and it increases considerably for the oxides as compared to the metals.

In the present experiment, we have measured excitation-energy-dependence of Cu $L_{2,3}$ X-ray emission spectra of Cu, Cu_2O and CuO using synchrotron radiation in order to study the effect of chemical bonding in the excitation and deexcitation processes of inner-shell electrons of Cu metal and its oxides.

EXPERIMENT

The Cu (99.99 %) foil sample and sintered Cu_2O (99.9 %) and CuO (99.9 %) samples were commercially obtained. The spectral measurements in the Cu *L* region of these samples were performed at the beamline BL-8.0.1 for X-ray emission and fluorescence yield (FY) X-ray absorption measurements and at BL-6.3.1 for total-electron yield (TEY) X-ray absorption measurements.

In order to determine the excitation energies, XA spectra were measured by total electron-yields measurements. The incident photon current was continuously monitored using a gold mesh in

front on the sample to normalize the XE spectra.

RESULTS AND DISCUSSION

Cu $L_{2,3}$ X-ray emission (XE) spectra of Cu, Cu_2O and CuO spectra were measured at ten different excitation energies from 930~934 eV, at the L_3 threshold energy, up to energies as high as 990 eV, above the L_2 threshold energy. Figure 1 shows Cu $L_{2,3}$ XE spectra normalized to the integrated photon flux, excited at specific energies. The spectra were measured at 930~934 eV (L_3 threshold), at 950~952 eV (L_2 threshold), and at 990 eV (above the L_2 threshold). The relative intensity $L\beta_1/L\alpha_{1,2}$ significantly depends on the incident photon energy and the target. The intensity ratio for the Cu target is constant at any incident photon energy. On the other hand, those for the Cu_2O and CuO targets are the highest at the L_2 threshold energy, decrease abruptly just after the L_2 threshold energy, and then increase with the incident photon energy. This tendency is of interest from the view of the chemical effects on the excitation and deexcitation processes for inner-shell electrons.

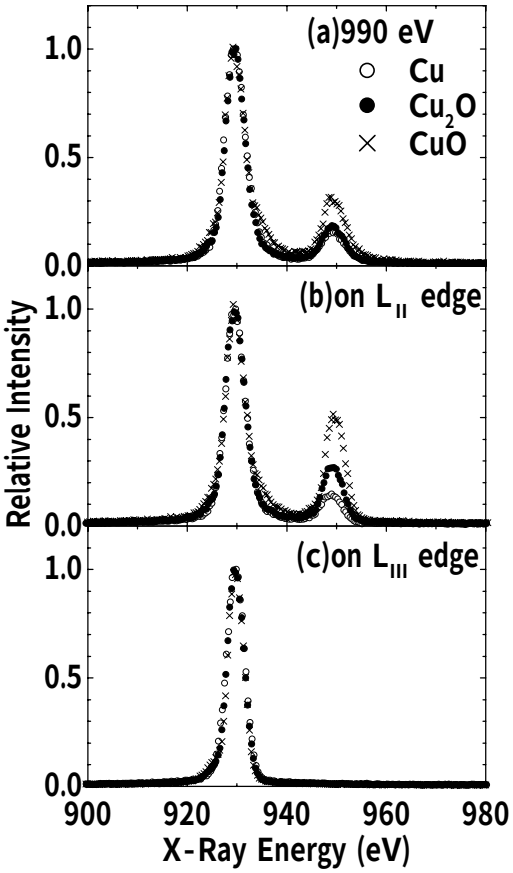

Figure 1. Comparison in the Cu L x-ray emission spectra of Cu, Cu_2O and CuO. Excitation energies are tuned at 990eV (a), L_2 (b) and L_3 (c) thresholds.

ACKNOWLEDGMENTS

We thank Dr. Jonathan Denlinger and Dr. Ponnusamy Nachimuthu for their helpful supports in performing X-ray emission and absorption measurements in BL-8.0.1 and BL-6.3.1, respectively. This work has been supported by the Hyogo Science and Technology Association and the US Department of Energy under Contract No. DE-AC03-76SF00098.

REFERENCES

1. V. Barnole, J.M. Mariot, C.F. Hague, C. Michel and B. Raveau, Phys. Rev. B **41**, 4262 (1990).
2. C. Sugiura, J. Phys. Soc. Jpn. **63**, 1835 (1994)
3. N. Wassdahl, J.-E. Rubensson, G. Bray, P. Glans, P. Bleckert, R. Nyholm, S. Cramm, N. Martensson and J. Nordgren, Phys. Rev. Lett. **64**, 2807 (1990).

4. K. Ichikawa, K. Jouda, S. Tanaka, K. Soda, M. Matsumoto, Y. Taguchi, T. Katsumi, O. Aita, H. Maezawa, Y. Azuma and H. Kitazawa, J. Electr. Spectr. Relat. Phenom. **78**, 183 (1996).
5. M. Magnuson, N. Wassdahl and J. Nordgren, Phys. Rev. B **56**, 12238 (1997).
6. D.W. Fischer, J. Appl. Phys. **36**, 2048 (1965).

This work was supported by the Hyogo Science and Technology Association and the US Department of Energy under Contract No. DE-AC03-76SF00098.

Principal investigator: Yasuji Muramatsu, Synchrotron Radiation Center, Kansai Research Establishment, Japan Atomic Energy Research Institute, 1-1-1 Kouto, Mikazuki, Hyogo 679-5148, Japan. E-mail: murama@spring8.or.jp. Telephone: +81-791-58-2601.

First Separate Measurements of the Nondipole Parameters γ and δ: Showcase Neon 2p Photoemission

O. Hemmers,[1] M. Blackburn,[2] T. Goddard,[2] P. Glans,[3] H. Wang,[4] S. B. Whitfield,[5]
R. Wehlitz,[6] I. A. Sellin,[7] and D. W. Lindle[1]

[1]Department of Chemistry, University of Nevada, Las Vegas, NV 89154-4003
[2]Advanced Light Source, Lawrence Berkeley National Laboratory, Berkeley, CA 94720, USA
[3]Department of Physics, Mid-Sweden University, Sundsvall S-85170, Sweden
[4]Department of Physics, Uppsala University, Box 530, S-751 21 Uppsala, Sweden
[5]Department of Physics and Astronomy, University of Wisconsin, Eau Claire, WI 54702-4004, USA
[6]Synchroton Radiation Center, University of Wisconsin, Stoughton, WI 53589, USA
[7]Department of Physics and Astronomy, University of Tennessee, Knoxville, TN 37996-1200, USA

INTRODUCTION

The familiar dipole approximation [i.e., exp(ik·r)≈1] limits photon interactions to purely electric-dipole (*E1*) effects. For photoemission processes, this approximation leads to the well-known expression for the differential photoionization cross section,

$$\frac{d\sigma(h\nu)}{d\Omega} = \frac{\sigma(h\nu)}{4\pi}\left[1+\frac{\beta(h\nu)}{2}\left(3\cos^2\theta-1\right)\right] \qquad (1)$$

which describes the angular distribution of photoelectrons ejected from a randomly oriented sample by 100 % linearly polarized light. Here, $\sigma(h\nu)$ is the partial photoionization cross section, and θ is defined as the angle between the outgoing electron and the photon polarization vector of the incoming, linear polarized light. In the dipole approximation, the parameter $\beta(h\nu)$ completely describes the angular distribution of photoelectrons, and all higher-order interactions, such as electric-quadrupole (*E2*) and magnetic-dipole (*M1*), are neglected. Over the past few decades, the dipole approximation has facilitated a basic understanding of the photoionization process in atoms and molecules, as well as the application of photoelectron spectroscopy to a wide variety of condensed-phase systems.

Beyond the dipole approximation, predictions and observations of high-photon-energy ($h\nu \geq 5$ keV) deviations from dipolar photoelectron angular distributions have enjoyed a successful history dating from the 1930's. Small deviations from expected dipolar angular distributions at photon energies between 1 and 2 keV were attributed qualitatively to the effects of higher-order photon interactions. These so-called *nondipole* effects in the angular distributions of photoelectrons, which are primarily due to first-order (*E2* and *M1*) corrections [*O(k)*] to the dipole approximation [i.e., exp(ik·r) ≈1 + ik·r], were later shown to lead to the expression

$$\frac{d\sigma(h\nu)}{d\Omega} = \frac{\sigma(h\nu)}{4\pi}\left[1+\frac{\beta(h\nu)}{2}\left(3\cos^2\theta-1\right)+\left(\delta(h\nu)+\gamma(h\nu)\cos^2\theta\right)\sin\theta\cos\phi\right] \qquad (2)$$

for 100 % linearly polarized light. The angle θ is defined above and φ is the angle between the photon propagation vector and the projection of the electron momentum vector into the plane perpendicular to the photon polarization vector. $\gamma(h\nu)$ and $\delta(h\nu)$ are the nondipole angular-distribution parameters attributable to first-order interactions only. Values of the first-order

nondipole parameters are determined by the strength of electric-quadrupole (E2) and magnetic-dipole (M1) photoionization amplitudes relative to the corresponding electric-dipole (E1) amplitudes. Expressions for γ and δ include *only* cross terms of the E2 and M1 amplitudes with the E1 amplitudes; "pure" quadrupole or magnetic-dipole interactions are not present in the first-order correction. Because the pure transitions are not included, the only manifestation of the first-order breakdown in the dipole approximation will be a change in the angular distribution of photoelectrons, specifically a forward/backward asymmetry relative to the photon propagation direction. The initial experiments motivated theoretical work, and more recent publications include quantitative predictions for a variety of atomic subshells. To date, all published experimental nondipole data did not separate the γ and δ parameters, except for the special case of n*s* photolines, where δ=0. The sum of γ and δ parameters is commonly expressed using the ζ parameter ($\zeta = \gamma + 3\delta$), which has been used for most of the experimental and recent theoretical work. The present work concentrates on the separate determination of γ and δ parameters for Ne 2*s* and 2*p* valence photoemission between 150 and 1200 eV and comparison to theoretical data.

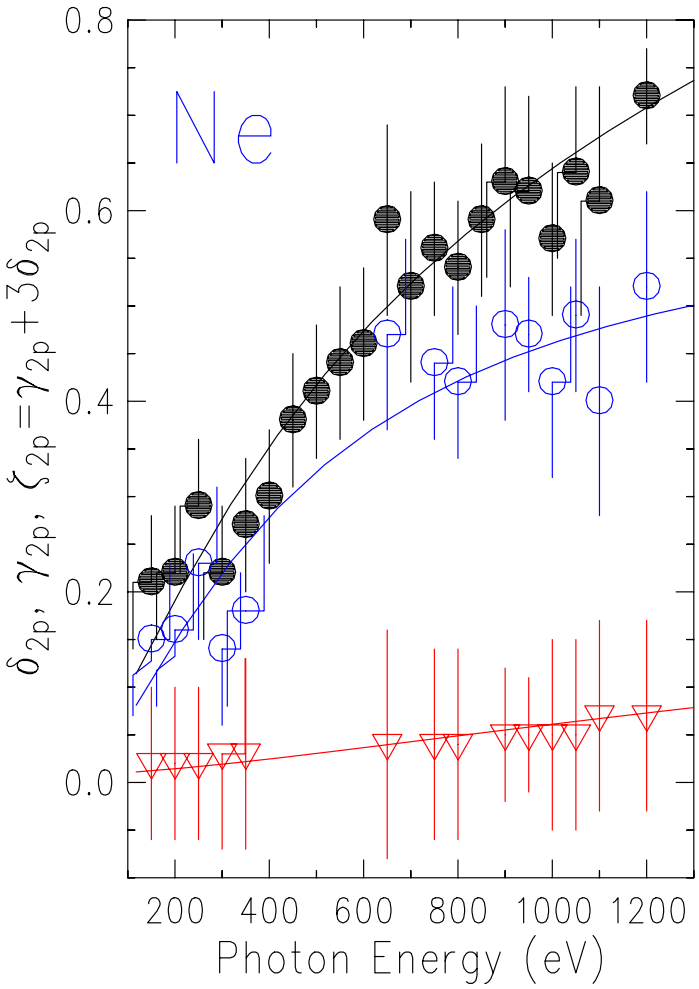

Figure 1. Photoelectron angular-distribution anisotropy parameter, δ (open triangles), γ (open circles), and ζ (filled circles), for Ne 2*p*. The theoretical data (solid line) are independent-particle calculations.

EXPERIMENTS

The present experiments were performed at the Advanced Light Source (ALS) of the Lawrence Berkeley National Laboratory on undulator beamline 8.0, which covers the 80-1300 eV photon-energy range. During the measurements the ALS operated at 1.9 GeV in two-bunch mode with a photon pulse every 328 ns. Four time-of-flight (TOF) electron analyzers, equipped with microchannel-plate detectors, collected spectra simultaneously at different angles. The interaction region was formed by an effusive gas jet intersecting the 0.4-mm-diameter photon beam. Energy resolution of the TOF analyzers with a focus size of 0.4 mm is about 1% of the final electron kinetic energy. A retarding voltage was used to slow the high-kinetic-energy electrons to a final kinetic energy of about 200 eV, thus maintaining the analyzer resolution at about 2 eV.

RESULTS

Figure 1 shows the experimental and theoretical data for the γ, δ, and ζ parameters for Ne 2*p* photoionization. All data agrees very well with theory but for certain energies it was not possible to satisfactorily separate the two parameters γ and δ and therefore the separated nondipole components γ and δ show less data than there are shown for ζ. Even though δ is very small for the Ne 2*p* photoionization it is not zero and clearly shows a trend to increase with photon energy. The relatively large error bars reflect a possible systematic uncertainty and not the statistical error of each point.

CONCLUSIONS

In summary, this is the first comprehensive study of dipole and nondipole angular-distribution parameters for atomic valence photoionization, in this case covering the photon-energy region from 150 eV to 1200 eV. For the first time the individual nondipole parameters γ and δ have been separately determined for a non-*s*-subshell photoline. The measured nondipole contributions to the photoelectron angular distributions agree very well with existing calculations. It is important to appreciate the fact that doing gas-phase and solid-state angle-resolved photoemission experiments can show sizeable nondipole effects below 1 keV; this work clearly demonstrates nondipole effects may need to be considered in photoemission measurements, *even* for $h\nu<1$ keV.

ACKNOWLEDGMENTS

The authors thank the staff of the ALS for their support, the IBM, LBNL, LLNL, University of Tennessee, and Tulane University collaboration for beam time at beamline 8.0. This work was supported by the National Science Foundation under Award No. PHY-9876996 and the Department of Energy. Work at the Advanced Light Source is supported by the Director, Office of Energy Research, Office of Basic Energy Sciences, Materials Sciences Division, of the U. S. Department of Energy under Contract No. DE-AC03-76SF00098.

Principal investigator: Dennis Lindle, Department of Chemistry, University of Nevada, Las Vegas, NV 89154-4003. Email: lindle@unlv.edu. Telephone: 702-895-4426.

This work has been accepted for publication in J. Electron Spectrosc. Relat. Phenom. (2002)

High Resolution Photoionization Measurements of Mg^+ and Al^+ Ions

A Aguilar[1,4], J B West[2], R A Phaneuf[1], H Kjeldsen[3], F Folkmann[3], J D Bozek[4], A S Schlachter[4] and C Cisneros[5]

[1]Department of Physics, MS220, University of Nevada, Reno, NV, 89557-0058, USA
[2]CLRC Daresbury Laboratory, Warrington WA4 4AD, UK
[3]Institute of Physics and Astronomy, University of Aarhus, DK-8000 Aarhus C, Denmark
[4]Advanced Light Source, Berkeley Lab, Berkeley, CA 94720, USA
[5]Centro de Ciencias Físicas, Universidad Nacional Autónoma de México, Apartado Postal 6-96, Cuernavaca 62131, México

INTRODUCTION

The measurements presented here were undertaken to provide high resolution data on the photoionization cross sections of the singly charged ions of Mg and Al. The initial measurements were made at the ASTRID storage ring at the University of Aarhus, where absolute cross sections were obtained, but the photon energy resolution was insufficient to identify all the spectral structure. This was particularly evident in regionswhere the $2p \rightarrow nd$ and ns resonances overlapped; configuration interaction was strong in these regions and it was difficult to make firm assignments. Beamline 10.0.1 at the ALS was able to provide resolution down to $\sim$5 meV in the photon energy region of interest, thereby revealing the underlying structure in the features observed previously [1, 2]. In this ALS experiment there was no requirement to make absolute measurements, since these had already been made on ASTRID. The present data could therefore easily be normalised to the earlier data to obtain oscillator strengths for the newly resolved structure.

EXPERIMENT

The measurements were made using the merged beam method, originally used for electron scattering cross sections [3] and later adapted for photoionization cross section measurements at the Daresbury Synchrotron Radiation Source [4]. At the ALS an ECR source was used to generate the ions of interest; it contained a metal vapour oven so that metallic ions could be produced. The ions were then magnetically selected and deflected electrostatically to merge with the path of the photon beam from a spherical grating monochromator over a length of $\sim$30 cm. The parent beam intensity was measured in a Faraday cup, and the ionised products were incident upon a stainless steel plate. The secondary electrons thus generated were detected by a microspherical plate; further details of the experimental equipment have been given by Covington *et al* [5].

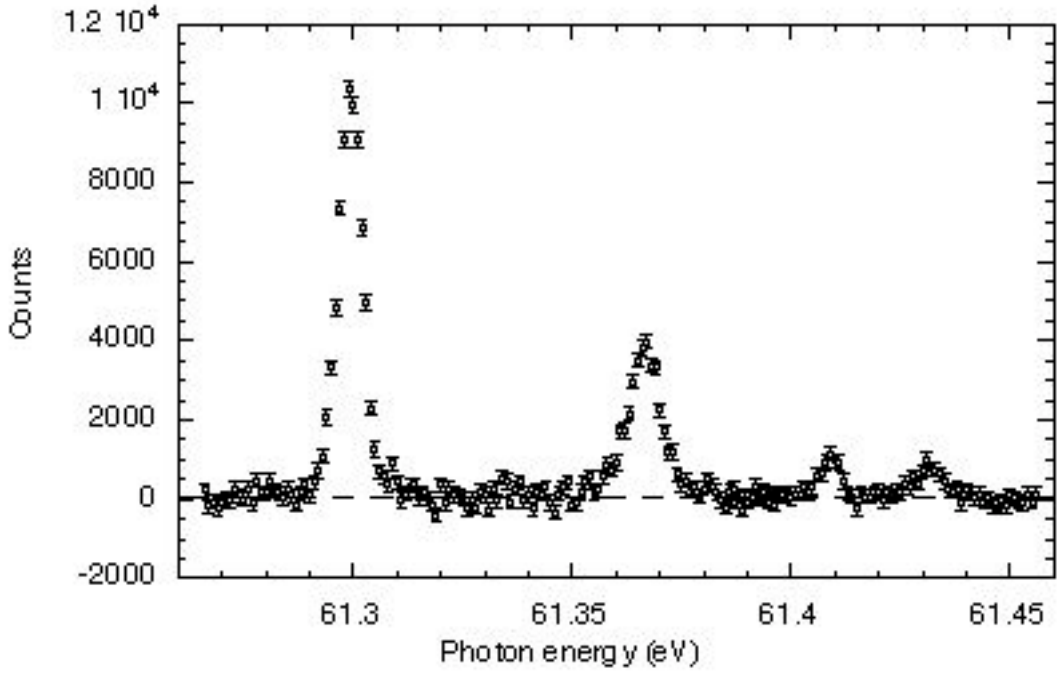

Figure 1: The photoionization spectrum of Mg^+.

RESULTS

For Mg^+ measurements were made over the photon energy range 61-68 eV, and a sample of these is shown in Fig. 1;these are preliminary results which have not been normalised and they are therefore relative. Four lines are evident, where previously one was observed. The lines at 61.30 and 61.37 are to be associated with transitions to the $2p^5 3s3d(^3D)\ ^2P$ levels of Mg^+, and the remaining two lines are probably due to transitions to the $2p^5 3s4s(^1S)$ levels. In Fig. 2 the corresponding region for Al^+ is shown. Rydberg series converging to the $2p^5 3s^2$ level of Al^{2+} at $\sim$92 eV are clearly evident.

Although a straightforward quantum defect analysis has been applied to the data above, the results are far from conclusive because of the large degree of configuration interaction taking place; the assumption of LS coupling may also be invalid. Even the above assignments must remain tentative until theoretical calculations are available; such calculations, using both the Multiconfigurational Hartree-Fock and R-matrix methods, are currently in progress.

ACKNOWLEDGMENTS

We are indebted to Andrew Mei of the LBL workshops, without whose skill in machining ceramic components for the metal vapour oven the experiments described here would not have been possible.

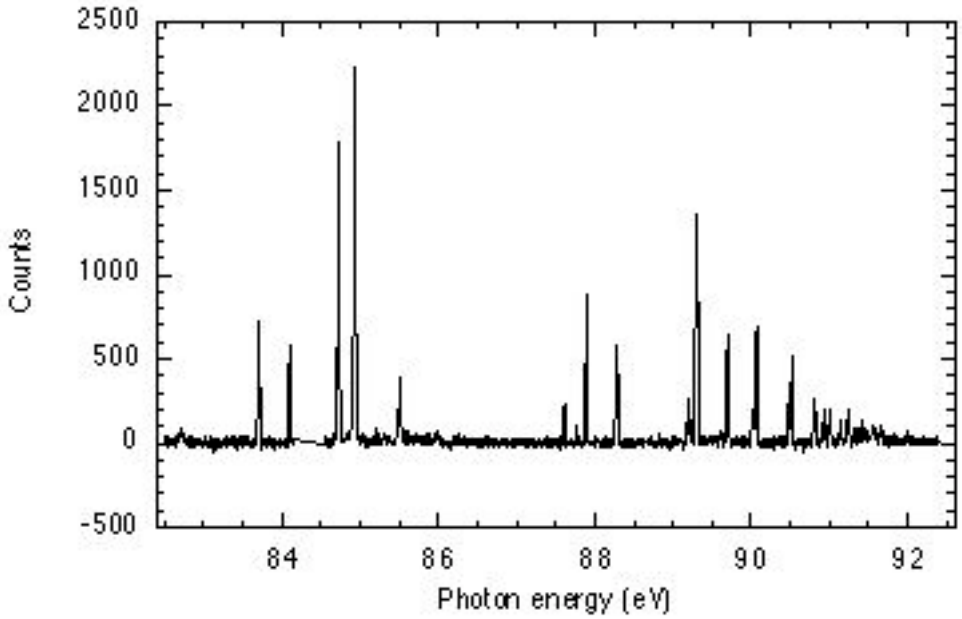

Figure 2: The photoionization spectrum of Al^+.

References

[1] H Kjeldsen, J B West, F Folkmann, H Knudsen and T Andersen T *J. Phys. B: At. Mol. Opt. Phys.* **33** 1403 (2000)

[2] J B West, T Andersen, R L Brooks, F Folkmann, H Kjeldsen and H Knudsen *Phys. Rev.* A **63** 052719 (2001)

[3] B Peart, J G Stevenson and K Dolder *J. Phys. B: At. Mol. Phys.* **6** 146 (1973)

[4] I C Lyon, B Peart, J B West and K Dolder *J. Phys. B: At. Mol. Phys.* **19** 4137 (1986)

[5] A R Covington *et al Phys. Rev. Lett.* **87** 243002 (2001)

This work was supported by the DOE, Contract No. DE-AC03-76SF00098, and in part by a research grant to JBW from the UK Engineering and Physical Sciences Research Council, by the DoE Divisions of Chemical Sciences, Geosciences, Physical Sciences and Materials Sciences, and by the DoE Facilities Initiative. Support was also provided by the Aarhus Center for Atomic Physics, through funding from the Danish National Research Foundation, and by DGAPA-UNAM.

Principal investigator: John B West, CLRC Daresbury Laboratory, Warrington WA4 4AD, United Kingdom. Email: j.b.west@dl.ac.uk.Telephone: +44 (0)1925 603241.

K-Shell Photodetachment of Li^-: Experiment and Theory

J. D. Bozek[1], A.A. Wills[2], G. Turri[1,2], G. Akerman[1], B. Rude[1], H.-L. Zhou[3], S. T. Manson[3], N.D. Gibson[4], C.W. Walter[4], L. VoKy[5], A. Hibbert[6], R.A. Phaneuf[7], S.M. Ferguson[2] and N. Berrah[2]

[1]Lawrence Berkeley National Laboratory, Advanced Light Source, Berkeley, Ca 94720
[2]Western Michigan University, Physics department, Kalamazoo, MI 49008
[3]Department of Physics and Astronomy, Georgia state University, Atlanta, GA 30309
[4]Department of Physics and Astronomy, Denison University, Granville, Ohio 43023
[5]DAMAP, UMR 8588 du CNRS, Observatoire de Paris 92195, Meudon Cedex, France
[6]Queen's University of Belfast, Belfast, BT7 1NN, United Kingdom
[7] University of Nevada, Reno, NV89557

Introduction

Investigation of the dynamics in negative ions provides valuable insights into the general problem of the correlated motion of electrons in many-particle systems, such as heavy atoms, molecules, clusters and solids. Photoexcitation and photodetachment processes of negative ions stand out as an extremely sensitive probe and theoretical test bed for the important effect of electron-electron interactions because of the weak coupling between the photons and the target electrons. In addition, negative ions present a severe theoretical challenge since the independent electron model is inadequate for even a qualitative description of their properties. Finally, studies of the properties of negative ions are needed since their production and destruction strongly affects systems such as dilute plasmas appearing in the outer atmospheres of stars. It has long been thought that electron correlations mainly involve the outer shell electrons of a negative ion, and only outer shell correlations were considered in theoretical calculations. However, new theoretical [1] works including core-valence and core-core effects has recently led to a better agreement with experiments. The present work shows how all the four electrons of Li^- are strongly affected by correlations. Li^-, ground state $1s^22s^2$ (^1S), is one of the simplest negative ions. However, its extended nuclear core, as compared to H^-, has a profound effect on the resonance structure. The lifting of the degeneracy of different l states with the same quantum number n opens up new decay channels. Outer-shell structures in the photodetachment cross section of Li^- have been extensively investigated experimentally [2,3] and they were well explained by theoretical calculations [4,5]. However, up until a very recent calculation [6] no published work in inner-shell photodetachment of negative ions was available other than the inner-shell theoretical work in He^- [7,8]. With the advent of 3rd generation synchrotron light sources with higher flux, brightness and resolution, it is now possible to investigate experimentally inner-shell processes in tenuous negative ion targets.

Experiment and theory

In this work, we report dramatic structure measured and calculated for the K-shell photodetachment of Li^-. This process leads to a core-excited state of Li which decays predominantly to the Li^+ ion. The measurements were performed at ALS Beamline10.0.1, used in tandem with the photon-ion experimental apparatus [9]. Li^- ions were produced using a cesium sputtering source (SNICS II) [10]. The Li^- ion beam was accelerated to 11 KeV, and a flux of 20-150 nA reached the interaction region. The ions were merged collinearly with the counterpropagating photon beam in a 30 cm long energy-tagged interaction region, producing neutral Li atoms and Li^+ ions. Li^+ ions were detected as a function of photon energy, using a photon resolution of 75 meV. The resulting signal was normalized to the primary Li^- ion beam and the incident photon flux. In the case of negative ions, merged experiments are a serious

challenge since the signal is very easily swamped by background noise due to stripping of negative ions with the residual gas (even though the background pressure in the interaction region was ~ 10^{-10} Torr) or with apertures in the ion beamline. In order to correct for the background ionization, the photon beam was chopped at 1 Hz and the photodetachment signal, corresponding to a relative cross section, was determined by subtracting the light-off signal from the light-on signal. The statistical error in the data was decreased by summing multiple sweeps of the photon energy of interest. The photon energies were calibrated separately using known resonance positions for neutral gasses and corrected for the Doppler shift, which amounts to about 108 meV for 60 eV photons. Calculations of the photodetachment of Li^- were performed using the R-matrix methodology which was enhanced to handle negative ions [11] and inner shells [12]. The discrete state input was generated with CIV3 [13]. A total of 29 target states were included in the close-coupling expansion: five $1s^2nl$ states, $n \leq 3$ and $l \leq 2$, and 24 1s2l3l', l=2,3, l'=0,1,2 core-excited states of Li. The cross section for Li^+ production for the Li^- photodetachment was obtained by summing all the cross sections for all of the channels leading to core-excited Li, since Li with a 1s-vacancy decays via Auger process virtually 100% of the time [14].

Results

The measured relative intensity was normalized to the magnitude of the calculated cross section at 62 eV. The calculated spectrum required only a small shift, +0.2 eV, to align to experimental data. It is interesting to note that this energy discrepancy is the same as that found in the case of photoionization of neutral Li [15]. The experimental and theoretical data are reported in Fig.1, where the neutral Li thresholds are reported.

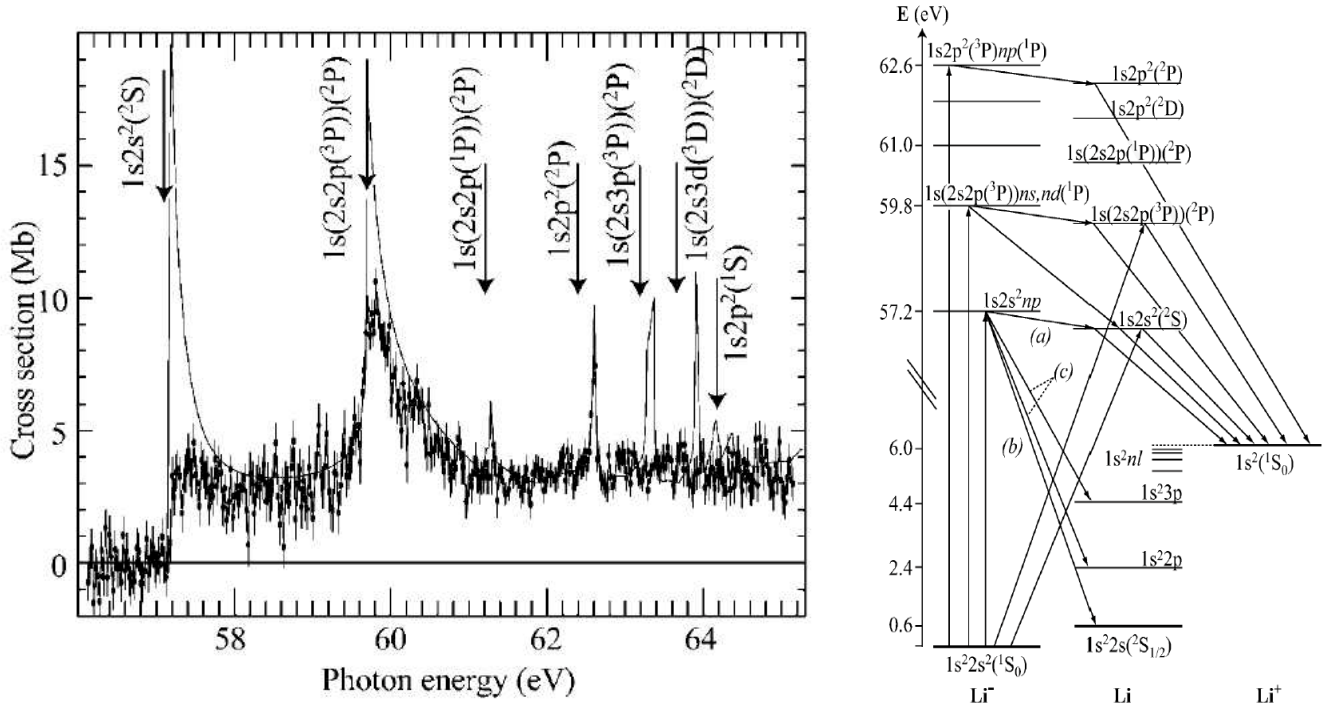

Fig.1 (left) Total double photodetachment cross section of Li^- giving rise to Li^+ in the vicinity of the 1s threshold. The solid curve is the R-matrix calculation and the dots with error bars are the experimental data normalized to the calculation at 62 eV. The arrows indicate the neutral Li thresholds. (right) Schematic energy level diagram (see text for details).

The experimental data clearly show three structures: first a step above the $1s2s^2\ ^2S$ threshold around 57.2 eV; second a shape resonance well defined by its sharp rise and decay tail above the second threshold $1s(2s2p\ ^3P)\ ^2P$; third a narrow resonance above the $1s2p^2\ ^2P$ threshold around 62.6 eV. Agreement between theory and experiment is quite good for the latter two structures, whereas the measured spectrum does not show the theoretically predicted shape resonance structure in the region above the first 1s detachment threshold. Li^+ can be produced in this energy region by autodetachment of the $1s2s^2np\ Li^-$ shape resonance to the core-excited $1s2s^2\ ^2S$ state of Li, which subsequently undergoes Auger decay to the ground state of Li^+, as labeled by process (a) in the energy level diagram of Fig, 1.

A similar process leads to the observed resonance structure above the second 1s threshold at 59.65 eV. In order for the $1s2s^2np\ Li^-$ states to produce Li^+, these states must be at higher energy than the first core-excited state of Li. As illustrated in the energy level diagram of Fig.1, this is the case for the $1s2s^2np$ excitations, which are found to be slightly above the $1s2s^2\ ^2S$ threshold for Li. Note that this situation is quite different from the case of neutral atoms, in the sense that there is not an infinite Rydberg series converging to each threshold. The lack of signal in the positive ion channel suggests that the $1s^2np$, $n>3$ states, omitted in the calculations, may play a significant role, since our results [16] are corroborated by an independent work [17].

It is surprising to find that the experiment was able to resolve and measure the predicted narrow structure above the $1s2p^2\ ^2P$ threshold around 62.6 eV, but not the predicted structures above the $1s(2s3p\ ^3P)^2P$ or $1s(2s3d^3D)^2D$ threshold above 63 eV or the weaker structure above the $1s(2s2p^1P)^2P$ around 61 eV. In the case of this last threshold, it may be that the signal to noise ratio is not sufficient to allow the observation of this weak structure. However the structure at 62.6 eV is expected to be stronger and narrower than the one at 63.2 eV, so at the moment we have no explanation for the discrepancy between experiment and theory in this region.

Conclusion

The first comparison between an experiment and theoretical K-shell study of the photodetachment of Li^- reveals dramatic structure, qualitatively and quantitatively unlike the same process in atomic Li or Li^+ ion. The calculations are able to predict the structures decaying to Li^+ in some cases, whereas the decay cross section is overestimated in the case of $1s(2s2p^3P)^2P$ and $1s2s^2\ ^2S$ thresholds. It is evident to us that although much of the essential physics of the inner-shell photodetachment problem is embodied in the calculation, there is still more to be understood, even in this simplest multishell negative ion.

Funding

DOE, Office of Science, BES, the NFS and NASA

Publication

N. Berrah *et al.*, K-Shell Photodetachment of Li^-: Experiment and Theory, Phys. Rev. Lett. 87, 253002 (2001).

References

[1] T. Andersen *et al.*, J. Phys. Chem. Ref. Data 28, 1511 (1999) and references therein

[2] G. Haeffler *et al.*, Phys. Rev. A 63, 053409 (2001) and references therein

[3] U. Berzinsh *et al.*, Phys. Rev. Lett. 74, 4795 (1995) and references therein

[4] C. Pan *et al.*, J. Phys. B 27, L137 (1994) and references therein

[5] E. Lindroth, Phys. Rev. A 52, 2737 (1995) and references therein

[6] H.-L. Zhou *et al.*, Phys. Rev. Lett. 87, 023001 (2001)

[7] D-S Kim *et al.*, J. Phys. B 30, L1 (1997)

[8] J. Xi and C.F. Fisher, Phys Rev. A 59, 307 (1999)

[9] A.M. Covington *et al.*, Phys. Rev. Lett. 87, 243002 (2001)

[10] R.D. Rathmell and G.A. Norton, Nucl. Instrum. Methods Phys. Res., Sect. B21, 270 (1987)

[11] H.-L. Zhou *et al.*, Phys. Rev. A 64, 012714 (2001)

[12] H.-L. Zhou *et al.*, Phys. Rev. A 59, 462 (1999)

[13] A. Hibbert, Comput. Phys. Commun. 9, 141 (1975)

[14] W. Bambynek *et al.*, Rev. Mod. Phys. 44, 716 (1972)

[15] S. Diehl *et al.*, Phys. Rev. Lett. 84, 1677 (2000)

[16] N. Berrah *et al.*, Phys. Rev. Lett. 87, 253002 (2001)

[17] B.H. Kjeldsen *et al.*, J. Phys. B 34, L353 (2001)

Principal investigator: Nora Berrah, Physics Department, Western Michigan University, Kalamazoo, MI 49008.
Telephone: (1) 616-387-4955. Fax: (1) 616-387-4939. Email: berrah@wmich.edu.

K-shell photoexcitation of carbon ions: lifetime of a K-shell vacancy

A. S. Schlachter[1], M. M. Sant'Anna[1,2], A. M. Covington[3], A. Aguilar[3], M. F. Gharaibeh[3], G. Hinojosa[4], R. A. Phaneuf[3], I. Alvarez[4], C. Cisneros[4], A. Müller[5], B. M. McLaughlin[6]
[1]Advanced Light Source, Ernest Orlando Lawrence Berkeley National Laboratory, University of California, Berkeley, California 94720, USA
[2]Pontificia Universidade Catolica do Rio de Janeiro, Rio de Janeiro 22452-970, Brazil
[3]Department of Physics, MS 220, University of Nevada, Reno, Nevada 89557-0058, USA
[4]Centro de Ciencias Fisicas, Universidad Nacional Autonoma de Mexico, Apartado Postal 6-96, Cuernavaca 62131, Mexico
[5]Institut für Kernphysik, Universität Giessen, D-35392, Giessen, Germany
[6]School of Mathematics and Physics, Queen's University of Belfast, Belfast BT71NN, UK

INTRODUCTION

Carbon is ubiquitous in nature and is the building block of life. The carbon atom in its various states of ionization has a small number of electrons, and is thus amenable to theoretical study. Given the importance of the carbon atom, it is surprising that there are few detailed measurements of inner-shell photoionization or photoexcitation processes, and that the lifetime of a K-shell vacancy in a free carbon atom is not experimentally known. The major difficulty is that free carbon atoms cannot readily be produced. In the present investigation we have measured photoexcitation of a C^+ ion rather than photoionization of a neutral carbon atom, producing the same state of C^+ as would be produced by direct photoionization of a neutral carbon atom. Photoexcitation of C^{2+} and C^{3+} has also been studied, both experimentally and theoretically.

LIFETIME OF A K-SHELL VACANCY

The lifetime of a K-shell vacancy in a free carbon ion (C^+) has been measured as part of a study of photoexcitation of K-shell electrons in carbon ions. The lifetime is determined by measuring the energy width of the resonance created by photoexcitation of a K-shell electron in the C^+ ion: the innermost 1s electron is promoted to the 2p shell, resulting in production of the $1s2s^22p^2\ ^{2,4}P$, ^2S, ^2D autoionizing states. The excited state of the C^+ ion produced in this experiment is identical to that produced by direct K-shell photoionization of the neutral carbon atom. Knowledge of such lifetimes is important for comparative studies of the autoionization widths for a K-shell vacancy in hydrocarbons and other carbon-containing molecules, where the molecular properties are known to affect the charge distribution and therefore the core-hole lifetimes and autoionization rates.

PHOTON-ION MERGED-BEAMS EXPERIMENT

A photon beam on beamline 10 is merged with a well-collimated energy- and charge-state-selected ion beam from a small accelerator [1]. The ion beam is charge-state analyzed after the interaction region: the primary ion beam is collected by a Faraday cup, while ions whose charge state has increased are detected and counted. The photon beam is time modulated to subtract ions which have changed their charge state in collision with background gas. All experimental parameters can be measured for determination of absolute cross sections; however, only relative cross sections have been measured in the present experiment.

RESULTS: ELECTRON SCREENING

Photon energy was scanned over the energy range where resonances are predicted by theory. Relative cross sections for photoexcitation of an admixture of ground-state and metastable C^+, C^{2+}, and C^{3+} beams are presented in Fig. 1. The insets show small peaks which would not be visible on the scale of the larger resonances. Experimental energies have been corrected for the Doppler-shift of the moving ions, and the energy scale has been determined relative to photoabsorption in CO. The large energy shift in the resonances with increasing charge state of the incident ion seen in Fig 1 is due to electron screening: there are fewer electrons on an ion in a higher charge state to pass between the nucleus and the K-shell electrons which reduce the nuclear charge felt by the K-shell electrons. Theoretical calculations using state-of-the-art techniques are in good agreement with the measurements. This comparison is valuable for benchmarking theory and for interpreting x-ray satellite data.

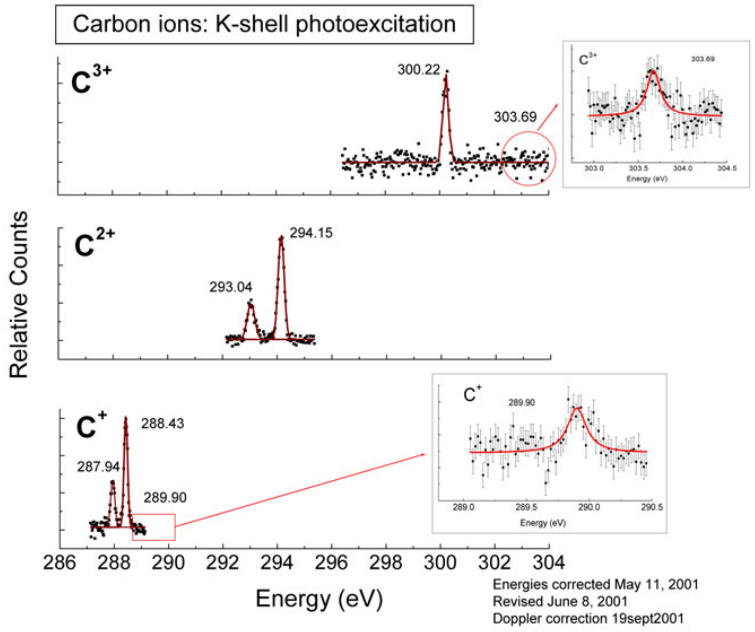

Figure 1. Experimental K-shell photoexcitation cross sections for C^+, C^{2+}, and C^{3+} ions. Relative cross sections are shown, for an admixture of ground-state and excited-state ions.

Natural linewidth can be measured in some cases by varying the spectral resolution of the incident photon beam, accomplished by changing the width of the entrance and exit slits of the monochromator. Data have been obtained for photoexcitation of C^+ ions with three different nominal spectral resolutions: 200 meV, 100 meV, and 50 meV. The resonance peaks were fit with a Voigt profile, which is a convolution of a Gaussian and a Lorentzian profile. The Gaussian width is instrumental, while the Lorentzian width is the natural lifetime width of the resonance. The fit was done on the two larger peaks, constrained to have the same Gaussian width for the same nominal resolving power. Results are shown in Fig. 2. The same value of lifetime linewidth was obtained for all three nominal spectral resolution values, providing confidence in the validity of the fitting process. The result is a width of 54 +/- 4 meV for the higher-energy peak and 102 +/- 10 meV for the lower-energy peak. It is interesting to note that the actual spectral resolution determined by the Gaussian width is better than the nominal resolution for relatively wide slits, but approaches the nominal width for the narrowest slits. This is because the undulator beam does not fill the entrance slit of the monochromator except for narrow settings of the entrance slit—which is the case for high spectral resolution.

The linewidth of a carbon-atom K-shell vacancy in a molecule is known to be greater than the theoretical linewidth of a free carbon atom due to molecular properties, e.g., charge distribution in the molecule. Coville and Thomas [2] and Carroll et al [3] list both theoretical and experimental values for a wide variety of carbon-containing molecules. A notable absence is that of an experimental value for a free carbon atom. (N.b., a carbon atom with a K-shell vacancy is, of course, a C^+ ion.) Two features are apparent from their work: the significant disagreement between experiment and theory; and the linewidth of a carbon K vacancy in all molecular species studied is significantly greater than the theoretical linewidth of a free carbon atom. The theoretical linewidth of a K-shell vacancy produced in a free carbon atom (thus in a C^+ ion) is 56 meV [2]. However, until now there have been no measurements of this linewidth. Furthermore, measurements of linewidths by photoionization of a molecular species are often complicated by post-collision interactions and other factors. The experimental method reported here, the production of the K-vacancy state of an atom by photoexcitation of the ion, does not have PCI, as there are no slow electrons to influence the lineshape. The lifetime of a K-shell vacancy is shorter in all molecules (the linewidth is greater) than in an isolated carbon atom. The present results are therefore significant in understanding vacancy-filling mechanisms in molecules. The measured lifetime agrees well with theory.

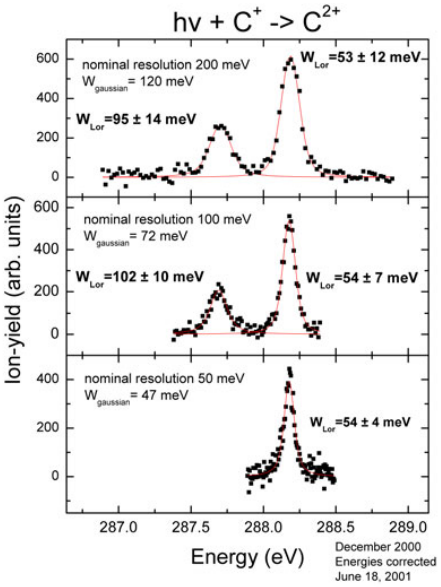

Figure 2. Experimental relative cross section for photoexcitation of C^+ ions, for three different values of nominal spectral resolution. The Gaussian width is the experimental resolution, the Lorentzian width is the lifetime width of each peak.

REFERENCES

[1] Covington et al, Phys. Rev. Letters **87**, 243002 (2001).
[2] Coville and Thomas, Phys. Rev. A **43**, 6053 (1991).
[3] Carroll et al, Phys. Rev. A **59**, 3386 (1999).

This work was supported by the Director, Office of Energy Research, Office of Basic Energy Sciences, Materials Science Division, of the U.S. Department of Energy under Contract No. DE-AC03-76SF00098, and the Division of Chemical Sciences, Geosciences and Biosciences

Principal investigator: R. A. Phaneuf, Department of Physics, University of Nevada, Reno NV 89557-0058. Email: phaneuf@physics.unr.edu. Telephone: 775 784-6818.

Mechanisms of Photo Double Ionization of Helium by 530 eV Photons

A. Knapp[1], A. Kheifets[2], I. Bray[3], Th. Weber[1], A. L. Landers[4], S. Schössler[1], T. Jahnke[1], J. Nickles[1], S. Kammer[1], O. Jagutzki[1], L. Ph. Schmidt[1], T. Osipov[5], J. Rösch[1,6], M. H. Prior[6], H. Schmidt-Böcking[1], C. L. Cocke[5] and R. Dörner[1]

[1] Institut für Kernphysik, Universität Frankfurt, August-Euler-Str. 6, D-60486 Frankfurt, Germany
[2] Research School of Physical Sciences and Engineering, Australian National University Canberra ACT 0200, Australia
[3]Centre for Atomic, Molecular and Surface Physics, Murdoch University, Perth, 6150 Australia
[4] Dept. of Physics, Western Michigan Univ., Kalamazoo, MI 49008
[5] Dept. of Physics, Kansas State Univ., Cardwell Hall, Manhattan KS 66506
[6] Lawrence Berkeley National Lab., Berkeley CA 94720

How does a single photon couple to two electrons in an atom? This question has been extensively discussed in the literature. Most of this discussion has been focused on the photo double ionization (PDI) of the helium atom which is the simplest two-electron-single-photon process. It is generally believed that at high photon energies the shake-off mechanism makes the largest contribution to PDI. The shake-off is a relaxation of the correlated initial state onto the new He^+ eigenstates after a sudden removal of one atomic electron. In contrast, close to the threshold, mainly one electron absorbs the photon and knocks out the second electron in an (e,2e) like collision (the process which is called in the literature the two-step-one, or TS1). The whole discussion on the PDI mechanisms is based solely on theory and on measured total cross sections. Differential data were available only in the regime of low energies, where the long range interaction between the electrons completely masks the signatures of the ionization mechanisms.

In this joint experimental and theoretical work we provide the first direct evidence for both mechanism by measuring the angular distributions of the photoelectrons by use of the COLTRIMS technique (Cold Target Recoil Ion Momentum Spectroscopy). The experiments have been performed at Bl. 4. They cover double ionization by linear and circular polarized light.

The following observations present the arguments for a two-step picture in which one electron absorbs the photon energy and its angular momentum and, subsequently, the second electron is either shaken-off or knocked out. The top panel of 1 shows the measured and calculated SDCS. It has a characteristic U-shape and peaks sharply at 0 eV

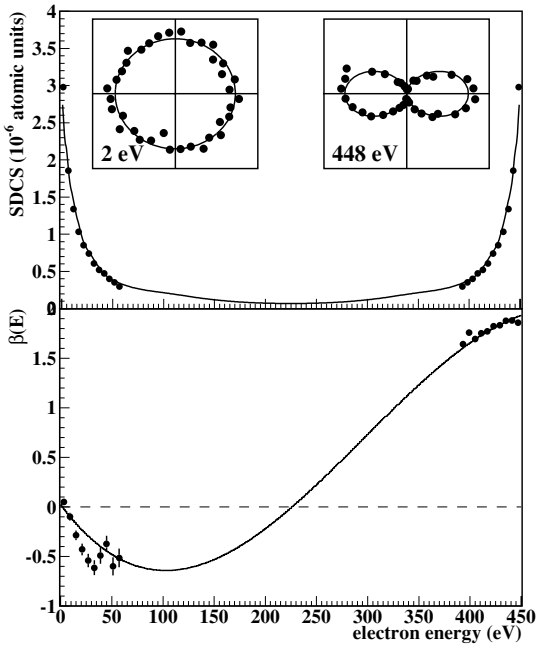

Figure 1: PDI of He at $\hbar\omega = 529$ eV. a) SDCS $d\sigma/dE$. The line is a CCC calculation. The insets show the DDCS $d\sigma^2/(d\Omega dE)$ at $E = 2$ eV and 448 eV. b) The asymmetry parameter β versus the electron energy.

and 450 eV. This run of the curve is in contrast to the SDCS close to the threshold which is almost flat. The bottom panel of 1 shows the measured and calculated β parameter. We find an angular asymmetry parameter $\beta \simeq 2$ for the very fast electrons and $\beta \simeq 0$ for the very slow electrons. Two examples of the experimental DDCS at $E = 2$ eV and 448 eV are shown in the insets together with the line obtained from CCC estimates of the SDCS and β. A very asymmetric energy sharing together with an angular asymmetry parameter $\beta \simeq 2$ for the fast electron indicate that the fast electron absorbs not only most of the photon energy but also its angular momentum. This directly suggests an interpretation of the PDI as a two-step process with the fast electron being the primary photoelectron. The very slow electrons are emitted isotropically at very low energies as expected for the shake-off, while β becomes slightly negative for higher energies indicating a major role of the TS1 at higher energies of the slower electron.

After establishing the validity of a two step picture we show now, that the second step of the PDI is dominated by the shake-off mechanism for very low energetic electrons (about 1 eV), while 30 eV electrons are created mainly by a binary (e,2e) like collision. In brief, the shake-off results in a almost isotropic, slightly backward directed emission of the slow electron with respect to the fast one, while any binary collision between the electrons leads to an angle of 90 deg between them.

The TDCS for electrons $E_2 < 3$ eV (figure 2b) has a pear-like shape peaked at 180° to the fast electron. Contrary to all TDCS reported at lower photon energies so far, these slow electrons show a significant intensity for parallel emission into the same direction. This is possible because of the very asymmetric energy sharing of the two electrons. The

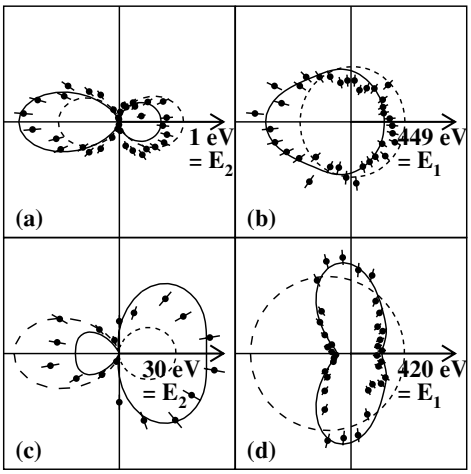

Figure 2: TDCS of the He PDI at 529 eV photon energy. In all panels the electrons are coplanar within $\pm 25°$, the polarization axis is horizontal. The direction and the energy of one of the two electrons is fixed as indicated by the number and the arrow, i.e. the slow electron is fixed in panels (a) and (c) and the fast electron is fixed in (b) and (d). The polar plots show the angular distribution of the complementary electron. The upper panels (a) and (b) are for the case $E_2 \simeq$ 2 eV; the lower panels have $E_2 \simeq$ 30 eV. The solid line is a full CCC calculation, the dashed line is a shake-off only CCC calculation. The measurements are normalized to the full CCC calculation.

solid line is a full CCC calculation which is in excellent agreement with the measurements.

The TDCS for electrons $E_2 \simeq 30$ eV (figure 2 c,d) are completely different from the low energy ones. We find emission of the electron into a narrow cone at 90° to the fast electron (figure 2 d). An angle of 90° between the electrons is expected from a binary collision between the electrons.

ACKNOWLEDGMENTS

Many thanks to E. Arenholz and T. Young and the staff of the ALS extraordinary support during our beam time. R. D. acknowledges many enlightening discussions with J. Berakdar, A. Becker and S. Keller.

This work was supported in part by BMBF, DFG, the Division of Chemical Sciences, Geosciences and Biosciences Division, Office of Basic Energy Sciences, Office of Science, U. S. Department of Energy and the Director, Office of Science, Office of Basic Energy Sciences. The computations were performed at the National Facility of the Australian Partnership for Advanced Computing. R. D. was supported by the Heisenberg Programm der DFG. A. K. and Th. W. thank Graduiertenförderung des Landes Hessen for financial support.

Principal investigator: Reinhard Dörner, Institut fuer Kernpyhsik, August Euler Str. 6, D-60486 Frankfurt, Germany, email: doerner@hsb.uni-frankfurt.de, phone: 049 69 798 24218

MIRRORING DOUBLY EXCITED RESONANCES IN NEON

S.E. Canton[1,2], A.A. Wills[2], T. W. Gorczyca[2], M. Wiedenhoeft[2],
E. Sokell[3], J.D. Bozek[1], G. Turri[1,2],Ximao Feng[2], and N. Berrah[2]
[1] Lawrence Berkeley National Laboratory, Advanced Light Source, University of California, Berkeley CA 94720.
[2] Department of Physics, Western Michigan University, Kalamazoo MI 49008.
[3] Department of Experimental Physics, University College Dublin, Ireland.

INTRODUCTION

The combination of high photon resolution and differential photoelectron spectroscopy techniques has allowed the discovery of new spectral features in the low-energy photoionization spectrum of neon. These resonances observed in the $2p^{-1}{}_{1/2,3/2}$ partial cross sections are attributed to LS forbidden doubly excited states with mirroring profiles [1]. The present results highlight the need for including relativistic interactions in the theoretical description of the photoexcitation process even for light systems.

EXPERIMENT

The experiment was performed on beamline 10.0.1 at the ALS. The apparatus consisted in two time of flight analyzers at 54.7^0 and 0^0 with respect to the electric field axis housed in a rotatable. The data was collected and displayed using a two dimensional acquisition technique consisting of recording data at closely spaced photon energies from which constant ionic spectra (CIS) were extracted as shown in Fig.1 to Fig.4. When the two photoelectron peaks corresponding to $2p^{-1}{}_{1/2,3/2}$ spaced by 97 meV are separated, the overall resolution of the CIS depends solely on the photon bandwidth. The spectral resolution was about 3 meV, close to the 10,000 resolving power obtainable at this beamline.

RESULTS

The present experiment follows up on previous work related to mirroring effects in Argon [2,3]. It gives the most detailed account of the resonant structure below the second ionization potential in neon up to date. In addition to the singly excited Rydberg series and the pronounced $2s^22p^4(^3P)3s(^2P)3p(^1P)$ excited state ,many new weak doubly excited states were observed. The strength of the experimental technique is fully demonstrated as most of the features can only be detected through the extraction of the corresponding branching ratio and at specific angles. Considering their energy position, they have been assigned with an LS forbidden triplet symmetry. For some of them, this is clearly confirmed by their mirroring profiles in the partial cross sections as shown in Fig.1 and Fig.2. The breakdown of LS coupling is further demonstrated by the branching ratio differing from the statistical value 2 by 10% throughout the whole spectral range. A complete calculation of the photoionization spectrum reproducing these highly correlated and spin-orbit induced resonances is still beyond the capabilities of available codes. However, it is hoped that this work will provide useful guidelines for further studies.

REFERENCES

[1] C.N. Liu, A.F Starace, Phys. Rev. A **59** R1731 (1999).
[2] S.E. Canton-Rogan, A.A. Wills, T.W. Gorczyca, M. Wiedenhoeft, O. Nayandin, C.N. Liu, and N. Berrah, Phys. Rev. Lett. **85**, 3113 (2000).
[3] C.D. Caldwell, S.B. Whitfield, and M.O. Krause, Mol. Phys, **98,** 1075 (2000).

This work was funded by the Department of Energy, Office of Science, Basic Energy Sciences, Chemical and Material Science Division, under the contract No. DE-FG02-92ER14299.

Principal investigator: Nora Berrah, Physics Dept., Western Michigan University, 616-387-4955, berrah@wmich.edu.

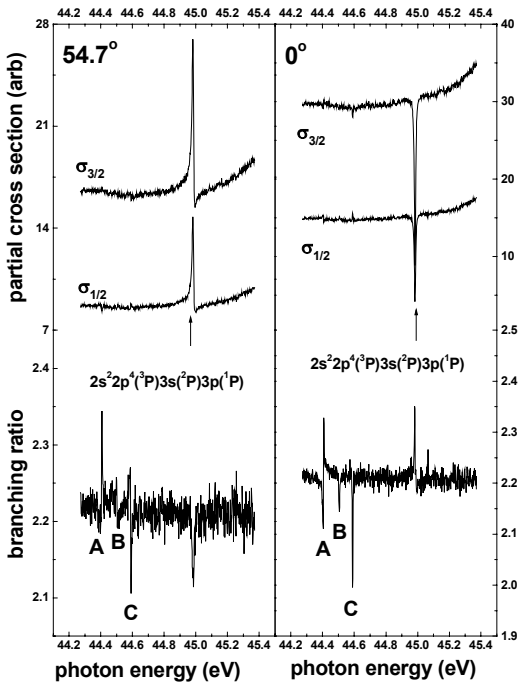

Fig.1: Partial differential cross sections meas-ured at the magic angle 54.7˚ and 0˚ with cor-esponding branching ratio in the vicinity of the first doubly excited state $2s^22p^4(^3P)3s(^2P)3p(^1P)$. Labels A, B, C indicate the position of the new doubly excited resonances.

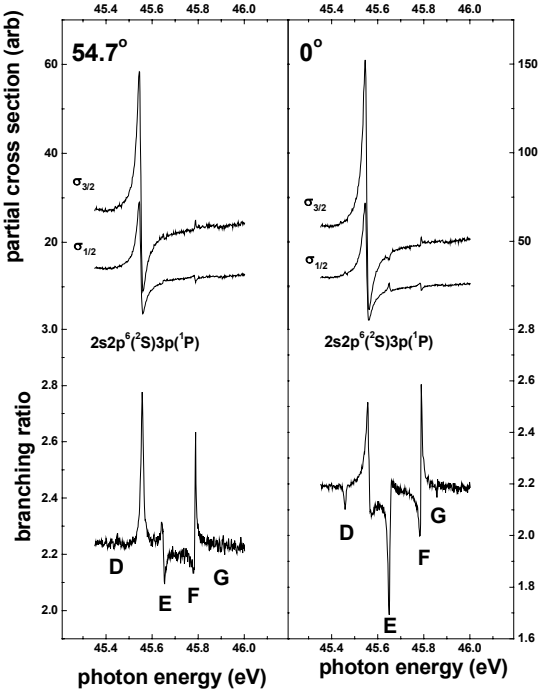

Fig.2: Partial differential cross sections measured at the magic angle 54.7˚ and 0˚ with corresponding branching ratio in the vicinity of the first singly excited state $2s2p^63p(^1P)$. Labels D, E, F, G indicate the position of the new doubly excited resonances.

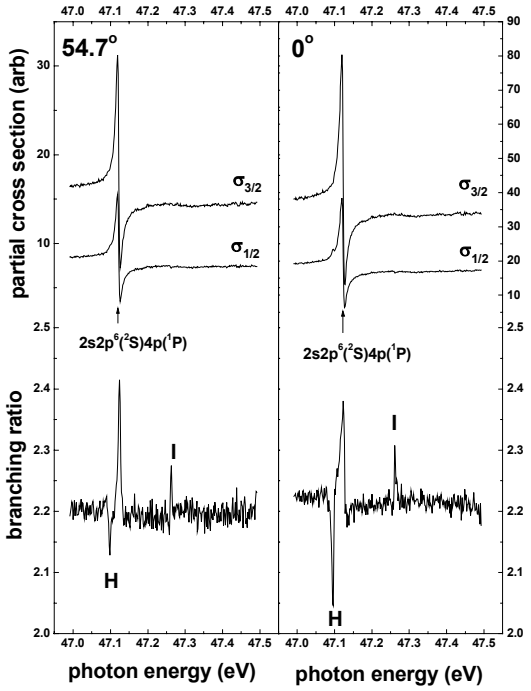

Fig.3: Partial differential cross sections measured at the magic angle 54.7˚ and 0˚ with corresponding branching ratio in the vicinity of the second singly excited state $2s2p^64p(^1P)$. Labels H, I indicate the position of the new doubly excited resonances.

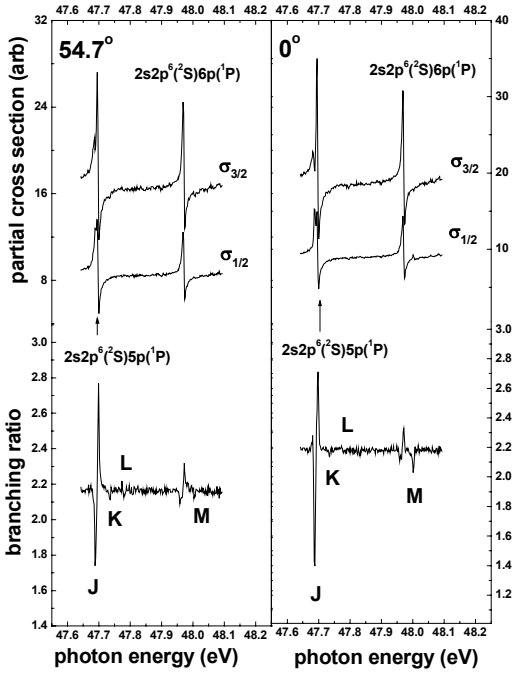

Fig.4: Partial differential cross sections measured at the magic angle 54.7˚ and 0˚ with corresponding branching ratio in the vicinity of the third and fourth singly excited state $2s2p^65p(^1P)$ and $2s2p^66p(^1P)$. Labels J, K, L, M indicate the position of the new doubly excited resonances.

Photoionization of C^{2+} ions

A. Müller[1], R. A. Phaneuf[2], A. Aguilar[2], M. F. Gharaibeh[2], A. S. Schlachter[3], I. Alvarez[4], C. Cisneros[4], G. Hinojosa[4] and B. M. McLaughlin[5]

[1]Institut für Kernphysik, Universität Giessen, D-35392 Giessen, Germany
[2]Department of Physics, MS 220, University of Nevada, Reno, NV 89557-0058, USA
[3]ALS, Lawrence Berkeley National Laboratory, Berkeley, CA 94720, USA
[4]Centro de Ciencias Físicas, UNAM, Apartado Postal 6-96, Cuernavaca 62131, México
[5]School of Math. and Physics, Queen's University of Belfast, Belfast BT7 1NN, UK

Photo*absorption* in the interstellar medium modifies the radiation spectrum of distant objects in the universe and thus complicates the interpretation of observations of such objects. Photo*ionization* of ions is an important mechanism for the production of highly charged ions in astrophysical plasmas exposed to hot sources of radiation. Ionization in such plasmas is usually balanced by low-energy electron-ion recombination. Because of their applied importance photon-ion and electron-ion collision processes have received long-standing interest by the plasma and astrophysics communities [1].

The pair of C^{2+} and C^{3+} ions is of particular interest for the understanding of astrophysical and man-made plasmas. Photoionization (PI) of C^{2+}

$$h\nu + C^{2+} \rightarrow C^{3+} + e \tag{1}$$

is the time-reversed (photo-)recombination (PR)

$$C^{3+} + e \rightarrow h\nu + C^{2+}. \tag{2}$$

Both reactions can proceed directly or in a multi-step fashion involving intermediate production of multiply excited autoionizing states. The indirect (resonant) PR channel is also called dielectronic recombination (DR). The principle of detailed balance, based on time-reversal symmetry, relates the cross sections of PI and PR on a state-to-state basis. Measuring one or the other of the two cross sections provides information about the time-reversed process. High resolution PR experiments with C^{3+} ions have been performed previously at heavy-ion storage rings [2, 3].

Here, we report on the first high-resolution PI experiments carried out with multiply charged ions at the Advanced Light Source (ALS). Our measurements are compared with state of the art theoretical calculations performed within the semi-relativistic Breit-Pauli R-matrix method. Absolute cross sections were determined at a number of selected energies by employing a suitable photon-ion merged beams technique. In addition, relative energy-scan measurements were carried out to cover a wide energy range in narrow energy

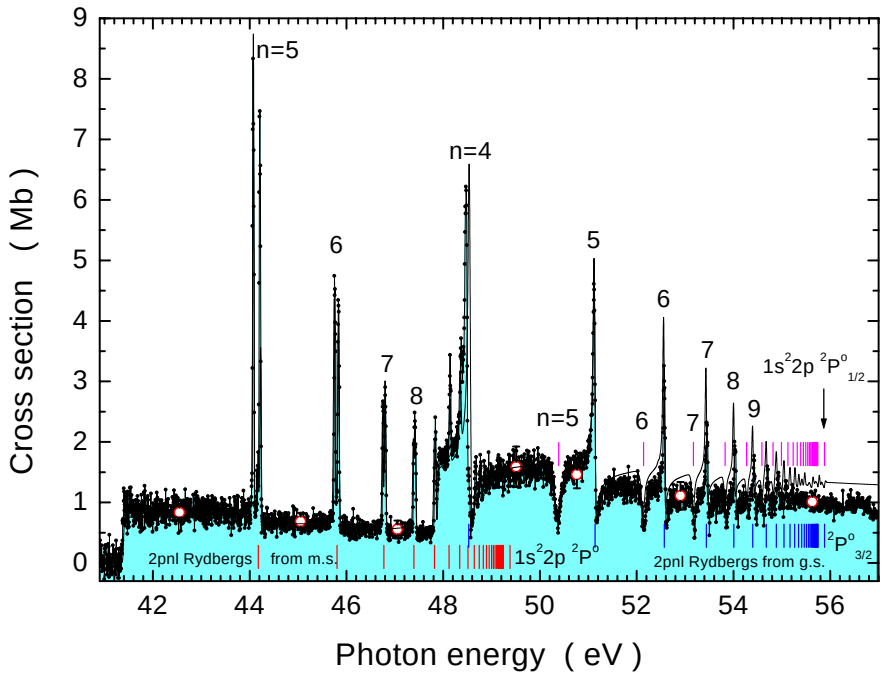

Figure 1: Measured and calculated cross sections for PI of C^{2+} ions. The energy-scan measurement is indicated by small dots connected by straight lines the area under which is shaded. The scan data were normalized to separate absolute PI cross section measurements (open circles with total error bars). The solid line represents the weighted sum of the R-matrix results assuming 60% of ground state (g.s.) ions in the primary beam, 30% in the $^3P_0$ and 5% each in the $^3P_1$ and $^3P_2$ metastable (m.s.) states. The theoretical result is almost indistinguishable from the measurements below 51 eV. The main Rydberg series of intermediate autoionizing states are indicated by vertical bars.

steps. The relative data were then normalized to the absolute cross sections. The C^{2+} target ions were produced with an all-permanent-magnet electron cyclotron resonance (ECR) ion source.

Fig. 1 shows an overview of the results obtained from the present experiment and theoretical calculations. The open circles represent the absolute cross sections. Total experimental uncertainties of these data are indicated by error bars. The normalized scan data are visualized by the shaded area. Theory is represented by a solid line obtained after convoluting the calculated results with a gaussian of 30 meV full width at half maximum. Excellent agreement between theory and experiment is obtained by assuming that the parent C^{2+} ion beam consisted of 60 % ground state ions and 40 % metastable ions (with 30% in the $^3P_0$ and 5% each in the $^3P_1$ and $^3P_2$ states). Almost perfect agreement of theoretical and experimental level energies is found.

Qualitatively, the PR experiments [3] show the same features as the PI data of Fig 1. The cross section is also dominated by ($2pnl$) Rydberg resonances. Near threshold, i.e.

just above the (PI) ionization limit of C^{2+} and just above zero electron energy in the e + C^{3+} (PR) measurement the energy resolution is comparable in both the PI and the PR experiments. The resolution is sufficient to determine the natural line width of some of the states involved. Also the energy scales of both experiments agree very well within uncertainties of the order of less than 15 meV. However, the time-reversed PR measurement produces cross sections which are roughly two orders of magnitude above the present PI results. This apparent discrepancy may be understood in terms of how the data are obtained in the different experiments and how the related cross sections are defined. The PI experiment was carried out with a mixed beam of ground state and metastable ions. PI including the resonance contributions can populate the ground state of C^{3+} and at energies above 49.380 eV (for the metastable beam component) and 55.883 eV (for the ground state component) also the first excited states of C^{3+} which thus contribute to the measured cross section. In the storage ring PR experiments, however, only ground state C^{3+} ions were investigated. So there are contributions in the measured PI cross section that are not included in the PR data. The opposite is also true. Due to the relaxed selection rules for electron-ion collisions PR can populate many more autoionizing resonances than photoexcitation, which is essentially restricted to electric dipole transitions. In addition the PR resonances can decay to excited C^{2+} states which were not accessible to the PI measurements. In the light of this discussion it becomes clear that detailed balance has to be applied with care; it is valid only on a state-to-state basis. Consequently, PI and PR experiments nicely complement rather than duplicate each other providing additional information that would not be accessible by just one of the measurements. Branching ratios for different decay paths (or excitation pathways in opposite direction) of multiply excited states can be quantified by the comparisons. For example, the relative probability of the two-electron one-photon de-excitation of the $C^{2+}(1s^2 2p4d\,^1P)$ resonance could be inferred to be about 7.9 %.

References

[1] M. J. Seaton, Y. Yu, D. Mihalas and A. K. Pradhan, Mon. Not. R. Astron. Soc. **266**, 805 (1994).

[2] S. Mannervik, D. deWitt, L. Engström, J. Lidberg, E. Lindroth, R. Schuch, W. Zong, Phys. Rev. Lett. **81**, 313 (1998).

[3] S. Schippers, A. Müller, G. Gwinner, J. Linkemann, A. A. Saghiri, A. Wolf, Astrophys. J. **555**, 1027 (2001).

This work is supported by NATO Collaborative Linkeage Grant PST.CLG.976362, Deutsche Forschungsgemeinschaft (DFG), the Department of Energy , Office of Basic Energy Sciences, by CONACyT and DGAPA (Mexico), NSF (USA), and by EPSRC (UK).

Principal investigator: Alfred Müller, Institut für Kernphysik, Strahlenzentrum der Justus-Liebig-Universität Giessen, D-35392 Giessen, Germany. Email: Alfred.Mueller@strz.uni-giessen.de. Telephone: xx49 641 99 15200

Photoionization of doubly charged scandium ions

S. Schippers[1], A. Müller[1], S. Ricz[2], M. E. Bannister[3], G. H. Dunn[4], J. Bozek[5], A. S. Schlachter[5], G. Hinojosa[6], C. Cisneros[6], A. Aguilar[7], A. Covington[7], M. Gharaibeh[7], and R. A. Phaneuf[7]

[1]Institut für Kernphysik, Justus-Liebig-Universität, 35392 Giessen, Germany
[2]Institute of Nuclear Research (ATOMKI), H-4001 Debrecen, Hungary
[3]Physics Division, Oak Ridge National Laboratory, Oak Ridge, TN 37831, USA
[4]JILA, University of Colorado, Boulder, CO 80309-0440, USA
[5]Advanced Light Source, Lawrence Berkeley Laboratory, Berkeley, CA, USA
[6]Centro de Ciencas Fisicas, UNAM, Cuernavaca, Mexico
[7]Department of Physics, University of Nevada, Reno, NV 89557, USA

INTRODUCTION

Considering the fact that the ground state configuration of both neutral potassium and singly charged calcium is [Ar]4s, doubly charged scandium with its [Ar]3d ground state configuration is the simplest atomic system with an open 3d shell. It is even simpler than neutral scandium which in addition to the 3d electron has a closed $4s^2$ shell outside the argon core. Therefore photoionization (PI) of Sc^{2+} is fundamentally interesting, especially in view of the severe discrepancies between experimental [1] and theoretical [2] PI cross sections for neutral scandium in the region of $3p \rightarrow 3d$ excitations. For these excitations PI of Sc^{2+} can be represented as

$$\begin{array}{rcl} h\nu + Sc^{2+}(3s^2 3p^6 3d) & \rightarrow & Sc^{2+}(3s^2 3p^5 3d^2) \\ & \searrow & \downarrow \\ & & Sc^{3+}(3s^2 3p^6) + e^-. \end{array} \qquad (1)$$

Here the vertical arrow represents the intermediate doubly excited $3p^5 3d^2$ states decaying predominantly by autoionization via Super-Coster-Kronig transitions (vertical arrow), and the diagonal arrow represents the direct 3d PI channel. It is also possible to study the time reverse of Eq. 1, i. e. the photorecombination (PR) of a $Sc^{3+}(3p^6)$ ion with a free electron (e^-). Theoretically, on a state-to-state level, PI and PR cross sections are linked via the principle of detailed balance. It is evident that the study of both processes yields complementary information about the doubly excited intermediate states involved. Results of Sc^{3+} PR measurements, that have been conducted at the heavy-ion storage ring TSR of the Max-Planck-Institut für Kernphysik in Heidelberg, Germany, are already published [3]. Here, we report on first PI results obtained in August 2001 at the photon-ion research facility located at the ALS undulator beamline 10.0.1.

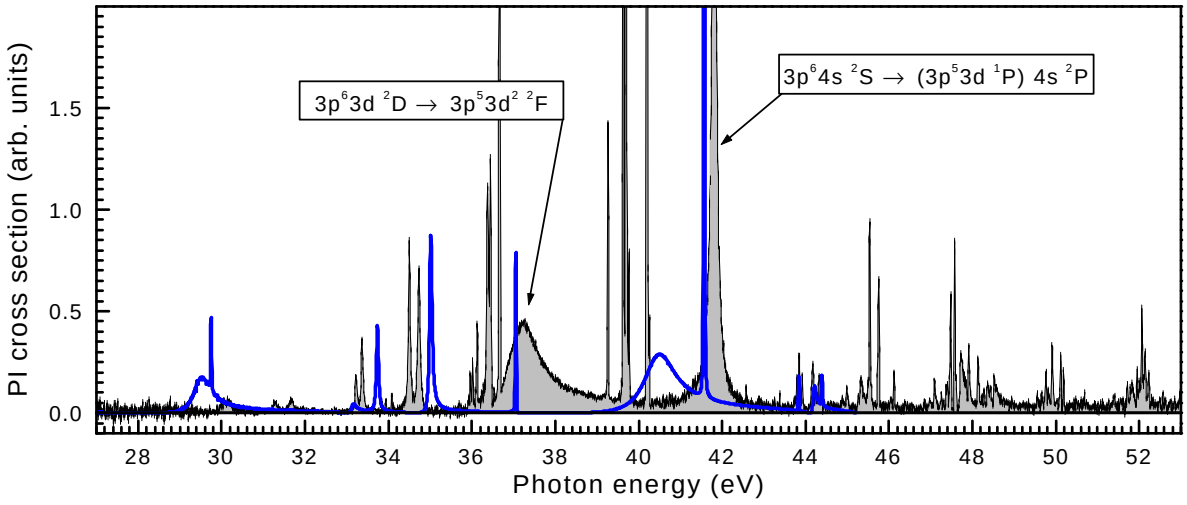

Figure 1: Part of the experimental spectrum (shaded curve) showing prominent resonances due to the excitation of the $3p^6 3d$ ground state and of the $3p^6 4s$ metastable state. The thick full line is the theoretical result of Altun and Manson [2].

EXPERIMENTAL PROCEDURE AND EXPERIMENTAL RESULTS

For the production of the Sc^{2+} ion beam, pieces of metallic scandium were vaporized inside an oven electrically heated to elevated temperatures. The Sc^{2+} ion beam was generated by ionizing the scandium atomic vapor by electron bombardment inside a compact electron cyclotron resonance (ECR) source. After having traveled through a bending dipole magnet serving for selecting the desired ratio of charge to mass, the ion beam was centered onto the counterpropagating monochromatized photon beam by applying appropriate voltages to several electrostatic ion beam steering devices. Electrical ion currents of up to 11 nA were available in the experiment. Behind the interaction zone the ion beam was deflected out of the photon beam direction by a second dipole magnet that also separates the ionized Sc^{3+} product ions from the Sc^{2+} parent ions. The Sc^{3+} ions were counted with nearly 100% efficiency with a single particle detector. From the measured Sc^{3+} count rate the PI cross section is readily derived by normalization on both photon flux and ion current.

The experimental photon energy range 23–68 eV encompasses the direct 3d and 3p photoionization thresholds. The experimental photo-ion spectrum is dominated by autoionizing resonances due to 3p excitations predominantly decaying via Coster-Kronig and Super-Coster-Kronig transitions (Fig. 1). The identification of the resonances is difficult. Only the most prominent resonance features can be identified with the aid of atomic structure calculations. The accurate calculation of resonance energies, widths and strengths for atomic systems with open 3d shells is a challenging task. The highly correlated nature especially of the doubly excited $3p^5 3d^2$ states requires large basis set expansions. Nevertheless, calculated resonance positions deviate by up to 3 eV from the measured resonance energies (Fig. 1).

Figure 2 shows resonances occuring in the energy range 36.62-36.72 eV. The exper-

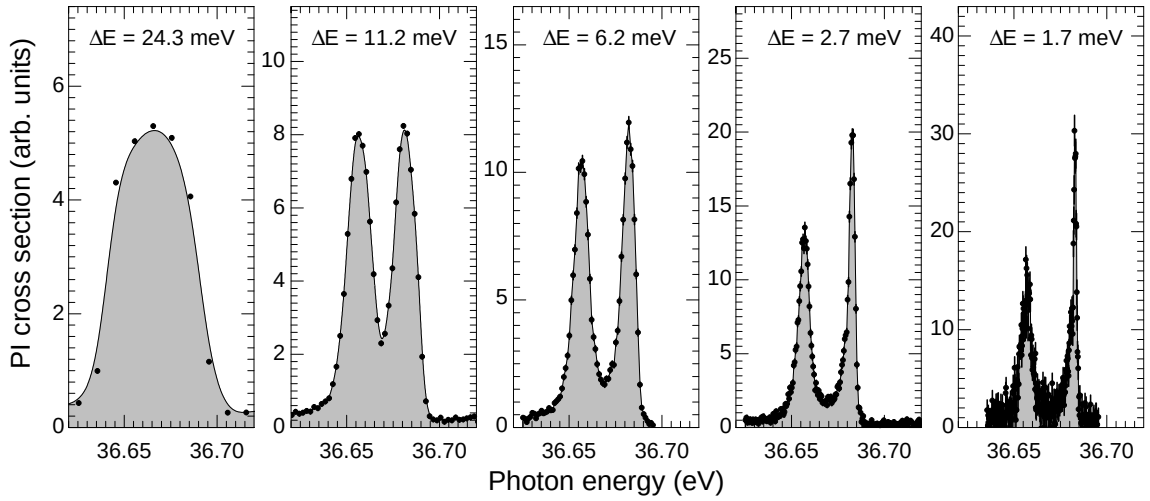

Figure 2: Influence of the experimental resolution on the measured photoionization cross section for a group of 3 resonances located around 36.67 eV.

imental photon energy spread was adjusted in a range of approximately 24 meV down to 1.7 meV by changing the width of the exit slit of the monochromator. At the highest resolution three individual resonances become visible. Likewise individual resonances located around $E \approx 40.2$ eV have been measured with an instrumental energy spread ΔE as low as 1.16 meV corresponding to a resolving power of $E/(\Delta E) \approx 35\,000$.

One complication with multiply charged ion beams extracted from an ECR ion source is the existence of a usually unknown amount of metastable ions in the beam. In the measured PI spectrum of Sc^{2+} (Fig. 1) we have identified resonances due to PI of the $Sc^{2+}(3p^6 3d\,^2D_{3/2})$ ground state as well as resonances due to PI of the $Sc^{2+}(3p^6 3d\,^2D_{5/2})$ and $Sc^{2+}(3p^6 4s\,^2S_{1/2})$ metastable states. A novel possibility to extract the fractions of metastable ions is provided by the comparison of the measured PI cross sections with the experimental PR cross sections of Schippers et al. [3] via detailed balance. The work is still in progress.

References

[1] S. B. Whitfield, K. Kehoe, R. Wehlitz, M. O. Krause, and C. D. Caldwell, Phys. Rev. A **64**, 022701 (2001).

[2] Z. Altun and T. Manson, J. Phys. B **32**, L255 (1999); Phys. Rev. A **59**, 3576 (1999).

[3] S. Schippers, S. Kieslich, A. Müller, G. Gwinner, M. Schnell, A. Wolf, M. Bannister, A. Covington, and L. B. Zhao, Phys. Rev. A (2002), in print.

This work was supported by the NATO Collaborative Research Grants CRG-950911 and CLG-976362.

Principal investigator: Alfred Müller, Institut für Kernphysik, Justus-Liebig-Universität, 35392 Giessen, Germany, Email: Alfred.Müller@strz.uni-giessen.de. Telephone: +49-641-99-15200.

Photoionization of Ne^+: an absolute benchmark for theory

A. M. Covington[1], A. Aguilar[1], I. Álvarez[2], J. D. Bozek, C. Cisneros[2], I. R. Covington[1], I. Dominguez[3], M. F. Gharaibeh[1], G. Hinojosa[1], B. M. McLaughlin[4], M. M. Sant'Anna[3], A. S. Schlachter[3], C. A. Shirley[1] and R. A. Phaneuf

[1]Department of Physics, University of Nevada, Reno, NV 89557-0058, USA
[2]Centro de Ciencias Físicas, Universidad Nacional Autonóma de México, Cuernavaca 62131, México
[3]Advanced Light Source, Lawrence Berkeley National Laboratory, Berkeley, CA 94720, USA
[4]School of Mathematics and Physics, Queens University, Belfast BT7 1NN, U.K.

The photoionization of ions is a fundamental process of importance in many high-temperature plasma environments, such as those occurring in stars and nebulae, as well as in inertial-confinement fusion experiments. Quantitative measurements of photoionization of ions provide precision data on ionic structure, and guidance to the development of theoretical models of multi-electron interactions. In addition, the opacity databases [1, 2] that are critical to the modeling and diagnostics of hot, dense plasmas consist almost entirely of untested coupled-state theoretical calculations based on the R-matrix method. High-resolution absolute photoionization cross-section measurements are therefore needed to benchmark these theoretical methods. Being the sixth-most abundant element in the universe, neon is significant in astrophysics, and therefore Ne^+ was selected for absolute measurements of photoionization cross sections to benchmark a state-of-the-art Breit-Pauli R-matrix theoretical calculation.

The experiments were performed on ALS beamline 10.0.1.2 using the ion-photon-beam (IPB) research endstation [3]. An energy-selected photon beam was merged over a path length of 29 cm with a highly collimated 6 keV Ne^+ beam produced in the hot-filament discharge ion source of the Cuernavaca ion gun apparatus. Two-dimensional intensity distributions of both beams were measured by rotating-wire beam profile monitors installed just upstream and downstream of the interaction region, and by a translating-slit scanner in the middle of the region. A downstream analyzing magnet separated the Ne^{2+} products from the parent Ne^+ beam. A spherical electrostatic deflector directed the Ne^{2+} products onto a biased stainless-steel plate, from which secondary electrons were detected by a microsphere-plate electron multiplier and counted. The absolute efficiency of the photoion detector (0.210 ± 0.005) was determined by measuring the photoion current with an averaging sub-femtoampere meter and comparing it to the measured count rate. The photon beam was mechanically chopped at 0.5 Hz to separate photoions from Ne^{2+} ions produced by stripping collisions of Ne^+ with residual gas in the ultra-high vacuum system. The photon energy and resolution were selected by a precision curved-grating monochromator. The undulator gap was set to maximize the photon intensity at each selected energy. The photon flux was recorded by a calibrated silicon X-ray photodiode, and was typically $2\text{-}3 \times 10^{13}$ photons/second at an energy of 45 eV and a bandwidth of 22 meV.

The absolute photoionization cross-section measurements taken at an energy resolution of 22 meV are compared in Figure 1 with the results of the *ab initio* Breit-Pauli R-matrix theoretical calculation. Two distinct threshold steps are evident at 40.866 eV and 40.963 eV, corresponding to non-resonant photoionization from the $^2P_{1/2}$ metastable state and the $^2P_{3/2}$ ground state, respectively. The calculation represents a sum of the cross sections for photoionization from the ground and metastable states, weighted by their statistical

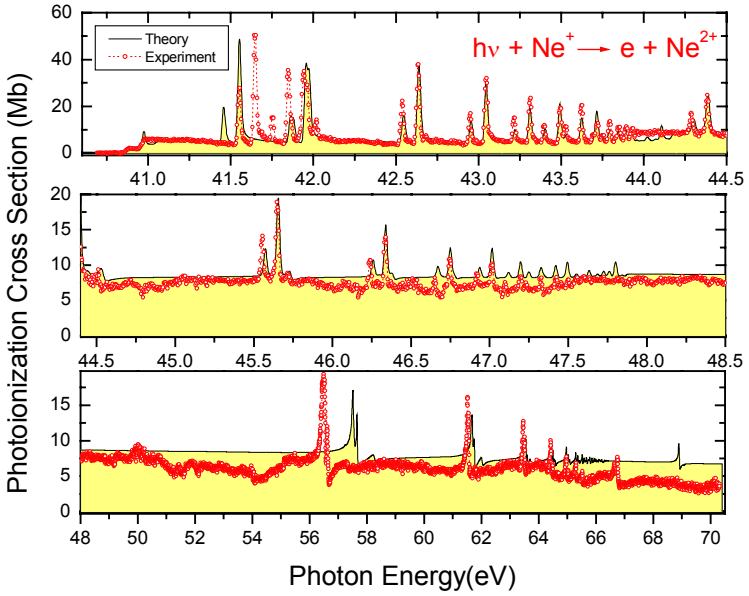

Figure 1. Comparison of absolute measurements (open circles connected by dashed lines) and Breit-Pauli R-matrix theory of McLaughlin (solid curve with shading) for photoionization of Ne^+. The theory has beeen convoluted with a Gaussian of 22 meV FWHM to simulate the bandwidth of the experiment.

weights (2/3 and 1/3, respectively). The calculated non-resonant cross section is almost indistinguishable from the absolute measurement in the energy range 41-44 eV, but diverges from the experiment at higher energies. The origin of the broad structures in the measurements above 44 eV may be interleaved series of $2s2p^4(^1S)ns\ ^2S$ window resonances similar to, but broader than, those observed by Caldwell et al [4] in photoionization of fluorine, which is isoelectronic with Ne^+. It is noteworthy that the predicted energy of the lowest-n resonance differs from experiment by about 100 meV, whereas most of the higher-n resonance energies are in agreement within 10 meV or better. The predicted energy of the $2s2p^5(^3P_2)3p$ resonance feature lies above the measured value of 56.49 eV by more than 1 eV, although the complex lineshapes are similar. A predicted sharp resonance near 69 eV is absent in the experimental data.

A detailed spectroscopic analysis of the resonance structure was performed in order to assign the observed features, which correspond to three Rydberg series of resonances converging to the $2s^22p^4\ ^1D_2$, $2s^22p^4\ ^1S_0$ and $2s2p^5\ ^3P$ excited states of Ne^{2+} at 44.167 eV, 47.875 eV and 66.292 eV, respectively from the ground state of Ne^+. The measurements along with their assignments are presented in Figure 2. The first two Rydberg series consist of pairs of sharp resonances separated by 97 meV that are distinguishable for autoionizing states with principal quantum numbers n as high as 25. The doubling corresponds to excitation from the ground-state and metastable-state components present in the ion beam. Resonances corresponding to the $2s2p^5(^3P)np$ series are sufficiently broad that components due to excitation from the ground and metastable states of Ne^+ are unresolved, except for the lowest 2p resonance near 42 eV.

Quantum-defect analyses were performed for each of the observed Rydberg series. The lowest members of the $2s^22p^4(^1D_2)nl$ and $2s^22p^4(^1S_0)nl$ Rydberg series were found to exhibit anomalous behavior with respect to their energy positions and relative resonance strengths, making it difficult to assign the features between 41.5 eV and 42.1 eV

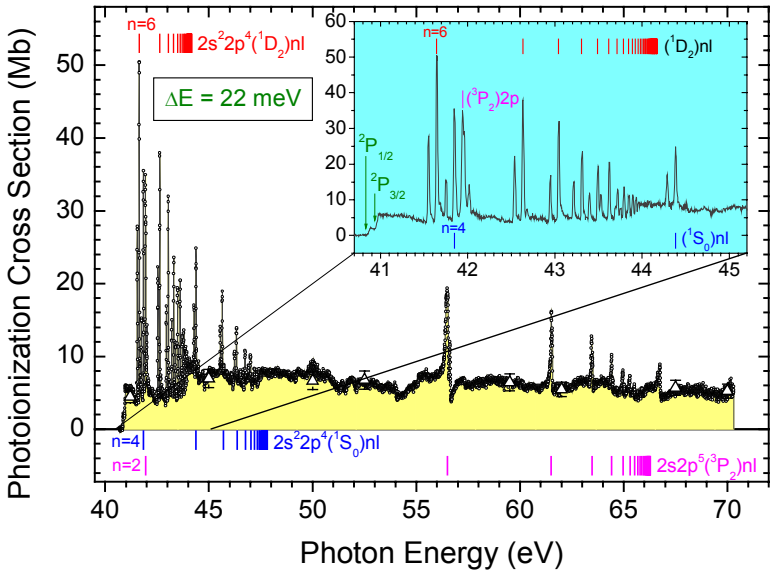

Figure 2. Absolute cross-section measurements for photoionization of Ne^{+} (triangles with error bars), to which broad photon energy scan taken at a resolution of 22 meV and a step of 4 meV was normalized. Three Rydberg series of resonances converging to excited states of Ne^{2+} are identified. The inset shows the measurements in the low-energy region on an expanded photon energy scale.

unambiguously. Each series converges to the known spectroscopic limit, independently verifying the photon energy calibration. This apparent breakdown of L-S-J coupling was not observed in photoionization of neutral fluorine [4]. It is surprising that such a dramatic change occurs suddenly along an isoelectronic sequence, motivating follow-up photoionization measurements on other members of this sequence (e.g. Na^{2+}).

REFERENCES

[1] W. Cunto, C. Mendoza, F. Ochsenbein and C. J. Zeippen, Astron. Astrophys. **275**, L5 (1993).

[2] C. A. Iglesias and F. J. Rogers, Astrophys. J. **464**, 943 (1996).

[3] A. M. Covington, A. Aguilar, I. R. Covington, M. F. Gharaibeh, C. A. Shirley, R. A. Phaneuf, I. Álvarez, C. Cisneros, G. Hinojosa, J. D. Bozek, I. Dominguez, M. M. Sant'Anna, A. S. Schlachter, N. Berrah, S. N. Nahar and B. M. McLaughlin, Phys. Rev. Lett. **87**, 243002 (2001).

[4] C. D. Caldwell and M. O. Krause, J. Phys. B Atom Molec. Phys. **27**, 4891 (1994); C. D. Caldwell, S. Benzaid, A. Menzel and M. O. Krause, Phys. Rev. A **53**, 1454 (1995).

The experimental work was supported by the Office of Basic Energy Sciences, Chemical Sciences, Geosciences and Biosciences Division, of the U. S. Department of Energy under contract DE-FG03-00ER14787 with the University of Nevada, Reno; by the Nevada DOE/EPSCoR Program in Chemical Physics and by CONACyT through the CCF-UNAM, Cuernavaca, Mexico. A.A. and M.M.SA. acknowledge support DGAPA-UNAM (Mexico) and CNPq (Brazil), respectively. The theoretical work was supported by ITAMP/Harvard-Smithsonian and by EPSRC (UK).

Principal Investigator: Ronald A. Phaneuf, Department of Physics /220, University of Nevada, Reno, NV 89557-0058. E-Mail: phaneuf@physics.unr.edu Telephone: 775-784-6818.

Soft x-ray emission spectroscopy of ions in solution

A. Augustsson[1], J.-H. Guo[1,3], D. Spandberg[2],
K. Hermansson[2] and J. Nordgren[1]

[1]Department of Physics, Uppsala University, Box 530, S-75121 Uppsala, Sweden
[2]Department of Materials Chemistry, Uppsala University, P.O. Box 538, S-75121, Uppsala, Sweden
[3]Advanced Light Source, Ernest Orlando Lawrence Berkeley National Laboratory, University of California, Berkeley, California 94720, USA

INTRODUCTION

Metal-ion transport in both aqueous- and polymer-solvent media involves continuos solvent-ligand exchange. Metal-ion coordination chemistry is therefore fundamental to these phenomena. The application of soft-x-ray absorption spectroscopy (SXAS) and soft-x-ray emission spectroscopy (SXES) to study wet samples has been hampered by the experimental difficulties of handling wet samples under high-vacuum conditions. Optical, infrared and Raman spectroscopies as well as magnetic resonance based methods are often used to determine the structure and the properties of these systems [1]. Here, we report the soft x-ray absorption and emission study of cations (Li^+, Na^+, K^+, Mg^{2+}, and Al^{3+}) in water solution.

Experiment

The experiments were performed at beamline 7.0.1 at the Advanced Light Source (ALS), Lawrence Berkeley National Laboratory. The beamline comprises a 99-pole, 5 cm period undulator and a spherical-grating monochromator [2]. In the liquid phase measurements, the incident photon beam and secondary emission penetrated a thin silicon nitride window of 100 nm in thickness. XAS spectra of liquid water were recorded in x-ray fluorescence yield. XES spectra were recorded using a high resolution grating spectrometer [3].

Cation-solvent interaction

The solvated cation interaction can be monitored by examining the spectra of the solvent. The advantage of this approach is that the restriction to cations no longer applies. For example, it can be used in studying what happens when salts of the alkali and alkaline earth metals are added to aqueous solvent. Series of spectra at different salts at a given concentration exhibit an isosbestic point. In the figure experimental data

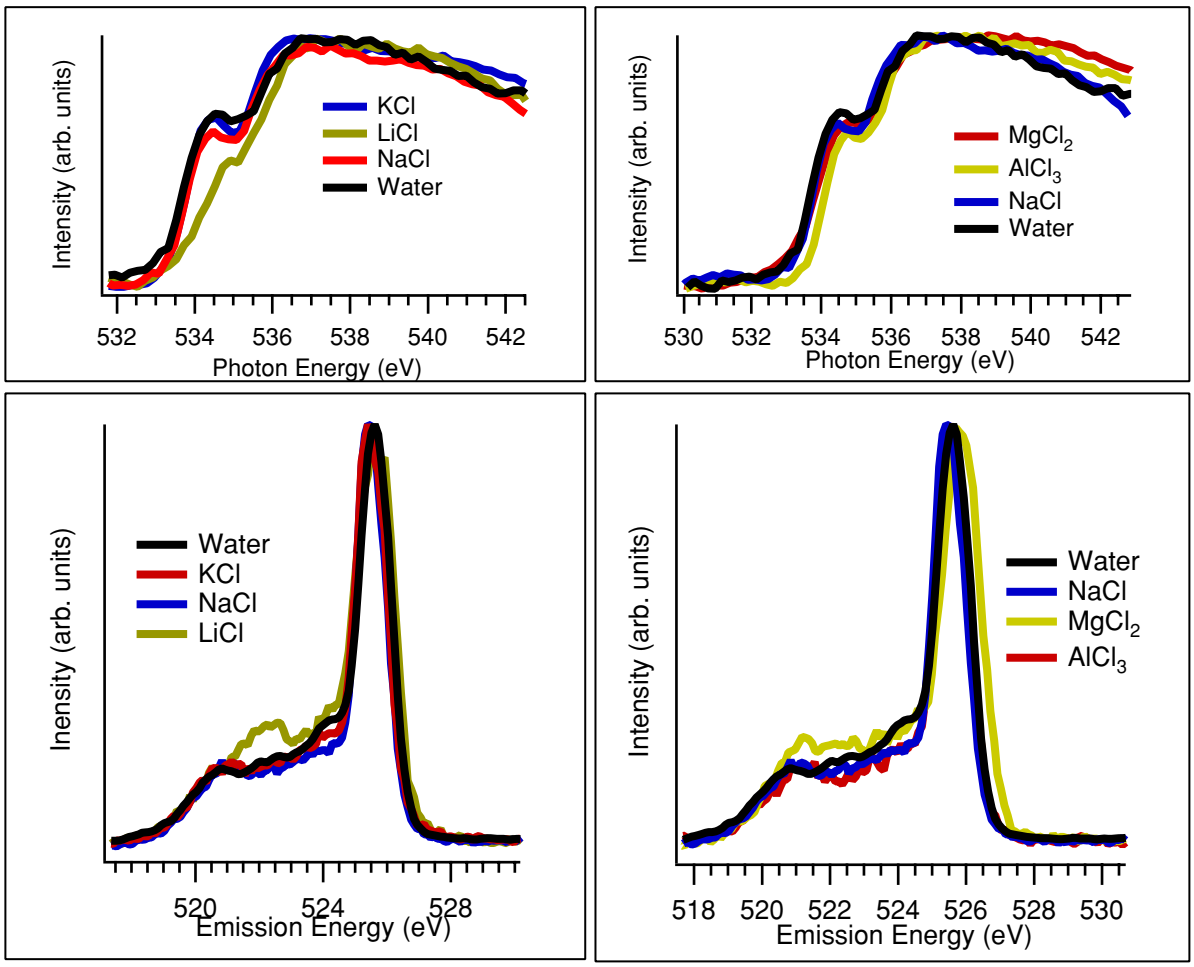

Figure 1: Top panels, O 1s XAS spectrum and bottom panels resonant O K-emission spectra of Ion solutions exited at the photon energy 534.5 eV

from ion-solutions are presented. Spectrum of pure water is also presented for comparison. The bottom panels shows the resonantly excited x-ray emission spectra, excited on the pre-edge in the absorption spectra at $\sim$ 534.5 eV (top panels). The left panel shows a comparison of O 1s spectra of solutions with ions of varying sizes and the right panel shows spectra varying charge. In the emission spectra one observe that spectrum of Na^+ and Al^{3+} solutions are similar while the emission spectrum of the Mg^{2+} solution show a broadened main peak, and some distinct differences at lower energies. Comparing Na^+ and K^+ solutions a small difference is observed, while the smaller Li ion shows a large spectral effect both in absorption and emission. We are presently working with theoretical interpretation, to achieve a full understanding of the data.

References

[1] Jean-Joseph Max and Camille Chapados, J. of Chem. Phys., 115, (2001), p. 2664

[2] T. Warwick and P. Heimann and D. Mossessian and W. McKinney and H. Padmore, Rev. Sci. Instrum. , 66, (1995), p.2037

[3] J. Nordgren and G. Bray and S. Cramm and R. Nyholm and J. -E. Rubensson and N. Wassdahl, Rev. Sci Instum. , 60, (1989), p.1690

This work was supported by the Swedish Research Council (VR), the Göran Gustafsson Foundation for Natural Science and Medicine, and the Swedish Institute.

Principal investigator: E. Joseph Nordgren, Department of physics, Uppsala University, Email: joseph@fysik.uu.se. Telephone: +46 18 4713554.